

Analysis of ECG signal for Detection of Cardiac Arrhythmias

A THESIS SUBMITTED IN PARTIAL FULFILLMENT
OF THE REQUIREMENTS FOR THE DEGREE OF

Master of Technology

in

Telematics and Signal Processing

By

JAYA PRAKASH SAHOO

Roll No: 209EC117



Department of Electronics and Communication Engineering

National Institute Of Technology, Rourkela

Orissa 769 008, INDIA

2011

Analysis of ECG signal for Detection of Cardiac Arrhythmias

A THESIS SUBMITTED IN PARTIAL FULFILLMENT
OF THE REQUIREMENTS FOR THE DEGREE OF

Master of Technology

in

Telematics and Signal Processing

By

JAYA PRAKASH SAHOO

Roll No: 209EC117

Under the Guidance of

Dr. Samit Ari

Assistant Professor



Department of Electronics and Communication Engineering

National Institute Of Technology, Rourkela

Orissa 769 008, INDIA

2011

Dedicated to

To My Parents, My brother and My Sister



NATIONAL INSTITUTE OF TECHNOLOGY
ROURKELA

CERTIFICATE

This is to certify that the thesis titled “**Analysis of ECG signal for Detection of Cardiac Arrhythmias**” submitted by **Mr. Jaya Prakash Sahoo** in partial fulfillment of the requirements for the award of Master of Technology degree **Electronics & Communication Engineering** with specialization in “**Telematics and Signal Processing**” during session 2009-2011 at National Institute Of Technology, Rourkela is an authentic work by his under my supervision and guidance.

To the best of my knowledge, the matter embodied in the thesis has not been submitted to any other university / institute for the award of any Degree or Diploma.

Date:

ROURKELA

Dr. Samit Ari

Assistant Professor
Dept. of Electronics & Comm. Engineering
National Institute of Technology
Rourkela-769008

Acknowledgement

I would like to express my gratitude to my supervisor **Prof. Samit Ari** for his guidance, advice and constant support throughout my thesis work. I would like to thank him for being my advisor here at National Institute of Technology, Rourkela.

Next, I want to express my respects to Prof. S.K. Patra, Prof. K. K. Mahapatra, Prof. S. Meher, Prof. S. K. Behera, Prof. Poonam Singh, Prof. A. K. Sahoo, Prof. D. P. Acharya, prof. S.K. Das and Prof. N. V. L. N. Murty for teaching me and also helping me how to learn. They have been great sources of inspiration to me and I thank them from the bottom of my heart.

I would like to thank all faculty members and staff of the Department of Electronics and Communication Engineering, N.I.T. Rourkela for their generous help in various ways for the completion of this thesis.

I would also like to mention the names of Manab, Dipak, Trilochan, Upendra and Sudhansu all the PhD student of DSP lab for helping me a lot during the thesis period.

I would like to thank all my friends and especially my classmates for all the thoughtful and motivating discussions we had, which encouraged me to think beyond the observable. I have enjoyed their companionship so much during my stay at NIT, Rourkela.

I am especially grateful to my parents for their love and support and would like to thank my parents for raising me in a way to believe that I can achieve anything in life with hard work and dedication.

Date:

Place:

Jaya Prakash Sahoo

Roll No: 209EC117
Dept of ECE, NIT, Rourkela

Table of Contents

ABSTRACT.....	i
LIST OF FIGURES.....	ii
LIST OF TABLES	iv
LIST OF ABBREVIATIONS	v
CHAPTER 1	1
Introduction	1
1.1 Electrocardiogram	2
1.2 The heart anatomy.....	2
1.3 Leads in ECG	3
1.4 ECG waves and interval.....	5
1.5 Noise in ECG Signal	7
1.5.1 Power line interferences	7
1.5.2 Baseline drift.....	7
1.5.3 Motion artifacts.....	8
1.5.4 Muscle contraction (EMG).....	8
1.6 Arrhythmias in ECG signal	9
1.6.1 Sinus Node Arrhythmias	10
1.6.2 Atrial Arrhythmias.....	10
1.6.3 Junctional Arrhythmias.....	11
1.6.4 Ventricular arrhythmias	12
1.6.5 Atrioventricular Blocks	13
1.6.6 Bundle Branch blocks.....	13
1.7 ECG Database	14
1.7.1 MIT-BIH Arrhythmias database.....	14
1.7.2 AAMI Standard	14
1.8 Motivation	15

1.9 Thesis Outline	16
References	16
CHAPTER 2	18
QRS Complex Detection	18
2.1 Introduction	19
2.2 Hilbert transform	19
2.3 Methodology	20
2.3.1 Filtering	21
2.3.2 Differentiation	21
2.3.4 Period calculation using autocorrelation	22
2.3.5 Sub window creation	23
2.3.6 High slope point detection using Hilbert transform	23
2.3.7 Adaptive threshold for noise removing	24
2.3.8 T wave discrimination	25
2.3.9 Second stage detector to find Q and S point	25
2.4 Result and discussion	25
2.5 Conclusion	28
References	28
CHAPTER 3	30
Feature Extraction of ECG Signal	30
3.1 Introduction	31
3.2 Methodology	31
3.2.1 RR-Interval Features	32
3.2.2 Heartbeat Interval Features	32
3.2.3 ECG Morphology Features	33
3.4 Simulation result	34
2.5 Conclusion	38

References	38
CHAPTER 4	40
Classification of Cardiac Arrhythmias	40
4.1 Introduction	41
4.2 Multilayer perception back propagation (MLP-BP) neural network	42
4.3 Radial basis function neural network (RBFNN)	43
4.4 Performance matrix	45
4.5 Classification Performance	46
4.6 Conclusion.....	51
References	52
CHAPTER 5	54
Conclusion and Future work	54
5.1 Conclusion.....	55
5.2 Future scope	56
5.3 References	56

ABSTRACT

Electrocardiogram (ECG), a noninvasive technique is used as a primary diagnostic tool for cardiovascular diseases. A cleaned ECG signal provides necessary information about the electrophysiology of the heart diseases and ischemic changes that may occur. It provides valuable information about the functional aspects of the heart and cardiovascular system. The objective of the thesis is to automatic detection of cardiac arrhythmias in ECG signal. Recently developed digital signal processing and pattern reorganization technique is used in this thesis for detection of cardiac arrhythmias. The detection of cardiac arrhythmias in the ECG signal consists of following stages: detection of QRS complex in ECG signal; feature extraction from detected QRS complexes; classification of beats using extracted feature set from QRS complexes. In turn automatic classification of heartbeats represents the automatic detection of cardiac arrhythmias in ECG signal. Hence, in this thesis, we developed the automatic algorithms for classification of heartbeats to detect cardiac arrhythmias in ECG signal.

QRS complex detection is the first step towards automatic detection of cardiac arrhythmias in ECG signal. A novel algorithm for accurate detection of QRS complex in ECG signal is proposed in chapter 2 of this thesis. The detection of QRS complex from continuous ECG signal is computed using autocorrelation and Hilbert transform based technique. The first differential of the ECG signal and its Hilbert transformed is used to locate the R-peaks in the ECG waveform. The autocorrelation based method is used to find out the period of one cardiac cycle in ECG signal. The advantage of proposed method is to minimize the large peak of P-wave and T-wave, which helps to identify the R-peaks more accurately. Massachusetts Institute of Technology Beth Israel Hospital (MIT-BIH) arrhythmias database has been used for performance analysis. The experimental result shows that the proposed method shows better performance as compared to the other two established techniques like Pan-Tompkins (PT) method and the technique which uses the difference operation method (DOM).

For detection of cardiac arrhythmias, the extracted features in the ECG signal will be input to the classifier. The extracted features contain both morphological and temporal features of each heartbeat in the ECG signal. Twenty six dimension feature vector is extracted for each heartbeat in the ECG signal which consist of four temporal features, three heartbeat interval features, ten QRS morphology features and nine T-wave morphology features.

Automatic classification of cardiac arrhythmias is necessary for clinical diagnosis of heart disease. Many researchers recommended Association for the Advancement of Medical Instrumentation (AAMI) standard for automatic classification of heartbeats into following five beats: normal beat (N), supraventricular ectopic beat (S), ventricular ectopic beat (V), fusion beat (F) and unknown beat (Q). The beat classifier system is adopted in this thesis by first training a local-classifier using the annotated beats and combines this with the global-classifier to produce an adopted classification system. The Multilayer perceptron back propagation (MLP-BP) neural network and radial basis function (RBF) neural network are used to classify the cardiac arrhythmias. Several experiments are performed on the test dataset and it is observed that MLP-BP neural network classifies ECG beats better as compared to RBF neural network.

LIST OF FIGURES

Fig. 1.1 The Heart conduction system [1].	3
Fig. 1.2 Precordial chest electrodes are normally placed on the left side of the chest [1].	4
Fig. 1.3 Schematic representation of normal ECG waveform.	5
Fig. 1.4 60 Hz Power line interference [6].	7
Fig. 1.5 Baseline drifts in ECG signal.	8
Fig. 1.6 Motion artifacts in ECG signal [6].	8
Fig. 1.7 Muscle contraction.	9
Fig. 1.8 (A) Normal sinus rhythm, (B) Sinus tachycardia	9
Fig. 1.9 Atrial arrhythmias, (A) Premature Atrial Contractions, (B) atrial tachycardia, (C) Atrial Flutter, (D) atrial fibrillation	11
Fig. 1.10 Junctional arrhythmias.	11
Fig. 1.11 Junctional arrhythmias (A) Premature Ventricular Contractions, (B) Ventricular Tachycardia, (C) Ventricular Fibrillation [1].	12
Fig. 0.12 Atrioventricular Blocks (A) first degree AV block, (B) Second degree AV block, (C) Third degree AV blocks.	13
Fig. 1.13 Bundle Branch blocks.	13
Fig. 2.1 Block diagram representation of the proposed method for detection of QRS complex.	20
Fig. 2.2 ECG signal in the database MIT-BIH tape #100 in the range (0-1000) samples. (a) channel-1 output, (b) channel-2 output, (c) band pass filter output.	21
Fig. 2.3 Sample beats from ECG signal of tape #100 in MIT-BIH database (a) band pass filter output, (b) derivative output.	22
Fig. 2.4 (a) filtered signal in the database MIT-BIH tape #100 in range 0-3s, (b) shifted version of above signal with a time lag (step size) of 0.02s.	22

Fig. 2.5 Autocorrelation output between the signals of fig. 2.4. (a) and (b). The maximum amplitude shows where two signals are correlated. The position where amplitude is maximum shows the period of one cardiac cycle.	23
Fig. 2.6 The maximum peak of Hilbert transform output is the zero crossing of differentiation output.	24
Fig. 2.7 The detected QRS point of signal tape #100	28
Fig. 3.1 (a) after getting fiducial point (FP), the QRS onset and offset and t-wave offset points are found, b) after determining the FP nine samples of the ECG between FP-50 ms and FP + 100 ms and nine samples between FP+150 ms and FP+500 ms are extracted [7]	33
Fig. 3.2 Ten fixed interval morphology features of QRS complex (left) and nine fixed interval morphology features of T-wave (right) of tape#100 in MIT/BIH database	34
Fig. 4.1 General Structure of multilayer neural network.	43
Fig. 4.2 General structure of the radial basis function neural network.	44
Fig. 4.3 Block diagram representation of ECG beat classifier.	45

LIST OF TABLES

Table 1.1 Types of leads used in ECG monitoring	4
Table 1.2 Amplitude and duration of waves, intervals and segments [6], [7], [8] of ECG signal.	6
Table 1.3 Mapping the MIT-BIH arrhythmia database heartbeat types to the AAMI heartbeat classes [15]	15
Table 2.1 The result of the proposed method for the signals in MIT-BIH database	26
Table 2.2 The comparison of the proposed method with the Pan-Tompkins (PT) method and difference operation method (DOM).	27
Table 3.1 Feature groups considered in this study	32
Table 3.2 Cardiac arrhythmia beat types in MIT/BIH database	34
Table 3.3 Patient by patient report of each tape according to AAMI recommendation excluding the tape contains paced beat	37
Table 3.4 Beat summary of MIT-BIH heartbeat types	38
Table 4.1 ECG classes and representation of desired neural network output	46
Table 4.2 Comprehensive results for testing files of 24 records in MIT/BIH arrhythmia database	47
Table 4.3 Summary table of beat-by-beat classification of 24 records in MIT/BIH arrhythmia database	48
Table 4.4 Classification performance of 24 records in MIT/BIH arrhythmia database	48
Table 4.5 SVEB result for testing files of 14 records in MIT/BIH arrhythmia database using MLP	48
Table 4.6 VEB result for testing files of 11 records in MIT/BIH arrhythmia database using MLP	49
Table 4.7 SVEB result for testing files of 14 records in MIT/BIH arrhythmia database using RBF	49
Table 4.8 VEB result for testing files of 11 records in MIT/BIH arrhythmia database using RBF	50
Table 4.9 SVEB and VEB comparison result are based on 14 and 11 common testing records respectively	50
Table 4.10 VEB and SVEB comparison result are based on 24 common testing records	51

LIST OF ABBREVIATIONS

ECG	Electrocardiogram
MIT-BIH	Massachusetts Institute of Technology Beth Israel Hospital database
N	Normal beat
L	Left bundle branch block beat
R	Right bundle branch block beat
A	Atrial premature beat
a	Aberrated atrial premature beat
J	Nodal (junctional) premature beat
S	Supraventricular premature beat
V	Premature ventricular contraction
F	Fusion of ventricular and normal beat
e	Atrial escape beat
j	Nodal (junctional) escape beat
E	Ventricular escape beat
/	Paced beat
F	Fusion of paced and normal beat
Q	Unclassifiable beat
MLP-BP	Multilayer Perceptron back propagation
RBF	Radial Basis Function
NaN	Not a Number
N/A	Not Analysed
AAMI	Association for the Advancement of Medical Instrumentation

CHAPTER 1

Introduction

1.1 Electrocardiogram

Electrocardiogram (ECG) is a diagnosis tool that reported the electrical activity of heart recorded by skin electrode. The morphology and heart rate reflects the cardiac health of human heart beat [1]. It is a noninvasive technique that means this signal is measured on the surface of human body, which is used in identification of the heart diseases [2]. Any disorder of heart rate or rhythm, or change in the morphological pattern, is an indication of cardiac arrhythmia, which could be detected by analysis of the recorded ECG waveform. The amplitude and duration of the P-QRS-T wave contains useful information about the nature of disease afflicting the heart. The electrical wave is due to depolarization and re polarization of Na^+ and k^- ions in the blood [2].The ECG signal provides the following information of a human heart [3]:

- heart position and its relative chamber size
- impulse origin and propagation
- heart rhythm and conduction disturbances
- extent and location of myocardial ischemia
- changes in electrolyte concentrations
- drug effects on the heart.

ECG does not afford data on cardiac contraction or pumping function.

1.2 The heart anatomy

The heart contains four chambers that is right atrium, left atrium, right ventricle, left ventricle and several atrioventricular and sinoatrial node as shown in the fig1.1 [1]. The two upper chambers are called the left and right atria, while the lower two chambers are called the left and right ventricles. The atria are attached to the ventricles by fibrous, non-conductive tissue that keeps the ventricles electrically isolated from the atria. The right atrium and the right ventricle together form a pump to the circulate blood to the lungs. Oxygen-poor blood is received through large veins called the superior and inferior vena cava and flows into the right atrium. The right atrium contracts and forces blood into the right ventricle, stretching the ventricle and maximizing its pumping (contraction) efficiency. The right ventricle then pumps the blood to the lungs where the blood is oxygenated. Similarly, the left atrium and the left ventricle together

form a pump to circulate oxygen-enriched blood received from the lungs (via the pulmonary veins) to the rest of the body [4].

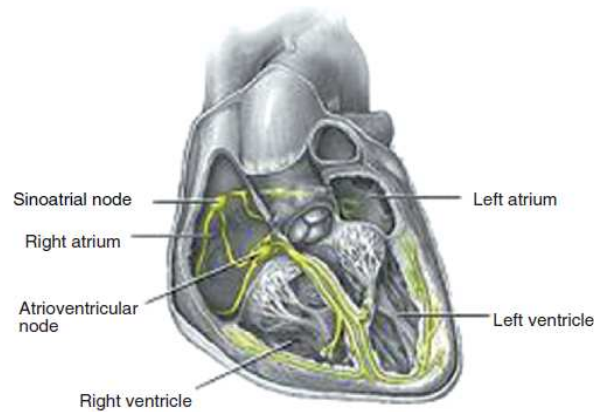


Fig. 1.1 The Heart conduction system [1].

In heart Sino-atrial (S-A) node spontaneously generates regular electrical impulses, which then spread through the conduction system of the heart and initiate contraction of the myocardium. Propagation of an electrical impulse through excitable tissue is achieved through a process called depolarization. Depolarization of the heart muscles collectively generates a strong ionic current [1]. This current flows through the resistive body tissue generating a voltage drop. The magnitude of the voltage drop is sufficiently large to be detected by electrodes attached to the skin. ECGs are thus recordings of voltage drops across the skin caused by ionic current flow generated from myocardial depolarisations[5]. Atrial depolarisation results in the spreading of the electrical impulse through the atrial myocardium and appears as the P-wave. Similarly, ventricular depolarisation results in the spreading of the electrical impulse throughout the ventricular myocardium.

1.3 Leads in ECG

The standard ECG has 12 leads: which includes 3 - bipolar leads, 3 - augmented unipolar leads and 3 - chest (precordial) leads. A lead is a pair of electrodes (+ve & -ve) placed on the body in designated anatomical locations & connected to an ECG recorder [3].

Bipolar leads: record the potential difference between two points (+ve & -ve poles).

Unipolar leads: record the electrical potential at a particular point by means of a single exploring electrode.

Leads I, II and III are commonly referred to bipolar leads as they use only two electrodes to derive a view. One electrode acts as the positive electrode while the other as the negative electrode (hence bipolar) [1].

Table 1.1 Types of leads used in ECG monitoring

Standard Leads	Limb Leads	Chest Leads
Bipolar leads	Unipolar leads	Unipolar leads
Lead I	AVR	V1
Lead II	AVL	V2
Lead III	AVF	V3
		V4
		V5

Einthoven leads:

Lead I: records potentials between the left and right arm,

Lead II: between the right arm and left leg, and

Lead III: those between the left arm and left leg

Goldberger leads are unipolar augmented limb leads in the frontal plane.

Unipolar Limb leads: (when the +ve terminal is on the right arm: aVR, left arm aVL, or left leg, aVF)

One lead connected to +ve terminal acts as the different electrode, while the other two limbs are connected to the -ve terminal serve as the indifferent (reference) electrode [5]. Wilson leads (V1–V6) are unipolar chest leads positioned on the left side of the thorax in a nearly horizontal plane. The indifferent electrode is obtained by connecting the 3 standard limb leads. When used in combination with the unipolar limb leads in the frontal plane, they provide a three-dimensional view of the integral vector.

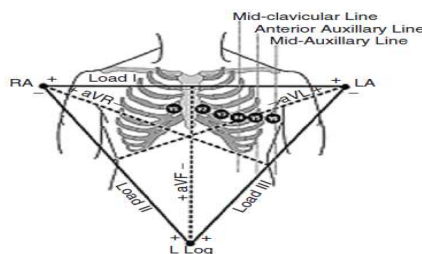


Fig. 1.2 Precordial chest electrodes are normally placed on the left side of the chest [1].

Chest (precordial) leads

V1: 4th intercostal space, right sternal edge.

V2: 4th intercostal space, left sternal edge.

V3: between the 2nd and 4th electrodes.

V4: 5th intercostal space in the midclavicular line.

V5: on 5th rib, anterior axillary line.

V6: in the midaxillary line.

To make recordings with the chest leads (different electrode), the three limb leads are connected to form an indifferent electrode with high resistances. The chest leads mainly detect potential vectors directed towards the back. These vectors are hardly detectable in the frontal plane [1]. Since the mean QRS vector is usually directed downwards and towards the left back region, the QRS vectors recorded by leads V1–V3 are usually negative, while those detected by V5 and V6 are positive [5]. In leads V1 and V2, QRS = -ve because, the chest electrode in these leads is nearer to the base of the heart, which is the direction of electronegativity during most of the ventricular depolarization process. In leads V4, V5, V6, QRS = +ve because the chest electrode in these leads is nearer the heart apex, which is the direction of electropositivity during most of depolarization [3].

1.4 ECG waves and interval

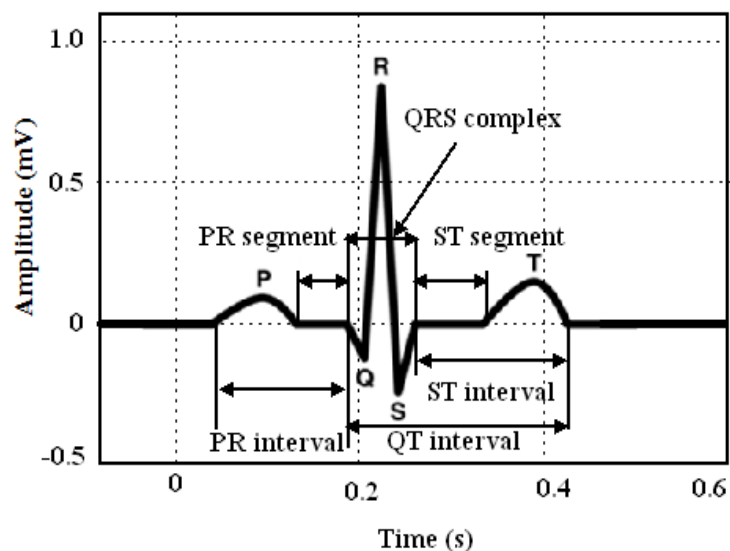


Fig. 1.3 Schematic representation of normal ECG waveform.

Waves

Representation

P wave

the amplitude level of this voltage signal wave is low (approximately 1 mV) and represent depolarization and contraction of the right and left atria [2].

A clear P wave before the QRS complex represents sinus rhythm.

Absence of P waves may suggest atrial fibrillation, junctional rhythm or ventricular rhythm.

It is very difficult to analyze P waves with a high signal-to-noise ratio in ECG signal.

QRS complex

The QRS complex is the largest voltage deflection of approximately 10–20 mV but may vary in size depending on age, and gender. The voltage amplitude of QRS complex may also give information about the cardiac disease [6].

Duration of the QRS complex indicates the time for the ventricles to depolarize and may give information about conduction problems in the ventricles such as bundle branch block.

T wave

Represents ventricular repolarization [3]

Large T waves may represent ischemia, and Hyperkalaemia

Table 1.2 Amplitude and duration of waves, intervals and segments [6], [7], [8] of ECG signal.

Sl. no.	Features	Amplitude (mV)	Duration (ms)
1	P wave	0.1-0.2	60-80
2	PR-segment	-	50-120
3	PR- interval	-	120-200
4	QRS complex	1	80-120
5	ST-segment	-	100-120
6	T –wave	0.1-0.3	120-160
7	ST-interval	-	320
8	RR-interval	-	(0.4-1.2)s

The Table1.2 shows features of P-wave, QRS complex and T wave in maximum amplitude and its duration. According to medical definition [7], the duration of each RR-interval is about 0.4-1.2s.

1.5 Noise in ECG Signal

Generally the recorded ECG signal is often contaminated by different types of noises and artifacts that can be within the frequency band of ECG signal, which may change the characteristics of ECG signal. Hence it is difficult to extract useful information of the signal. The corruption of ECG signal is due to following major noises:

1.5.1 Power line interferences

Power line interferences contains 60 Hz pickup (in U.S.) or 50 Hz pickup (in India) because of improper grounding [9]. It is indicated as an impulse or spike at 60 Hz/50 Hz harmonics, and will appear as additional spikes at integral multiples of the fundamental frequency. Its frequency content is 60 Hz/50 Hz and its harmonics, amplitude is up to 50 percent of peak-to-peak ECG signal amplitude [9]. A 60 Hz notch filter can be used remove the power line interferences [7].

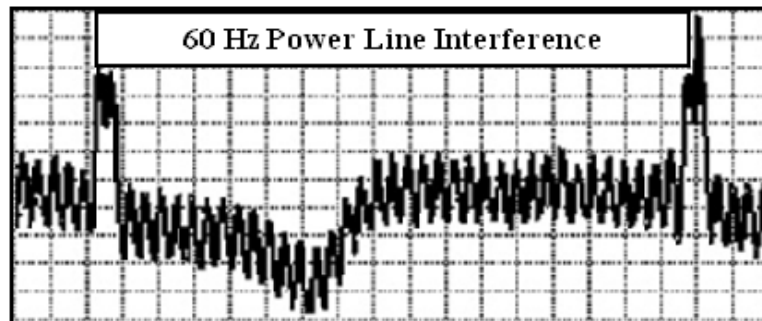


Fig. 1.4 60 Hz Power line interference [6].

1.5.2 Baseline drift

Base-line drift may be caused in chest-lead ECG signals by coughing or breathing with large movement of the chest, or when an arm or leg is moved in the case of limb-lead ECG acquisition [10]. Base-line drift can sometimes caused by variations in temperature and bias in the instrumentation and amplifiers. Its frequency range generally bellows 0.5 Hz. To remove baseline drift a high pass filter with cut-off frequency 0.5 Hz is used [7].

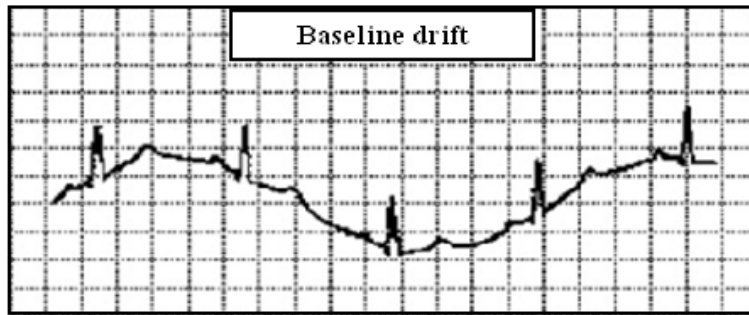


Fig. 1.5 Baseline drifts in ECG signal.

1.5.3 Motion artifacts

Motion artifacts are transient baseline change due to electrode skin impedance with electrode motion. It can generate larger amplitude signal in ECG waveform [7]. The peak amplitude of this artifact is 500 percent of Peak to Peak ECG amplitude and its duration is about 100 – 500 ms [9]. An adaptive filter can be used to remove the interference of motion artifacts.

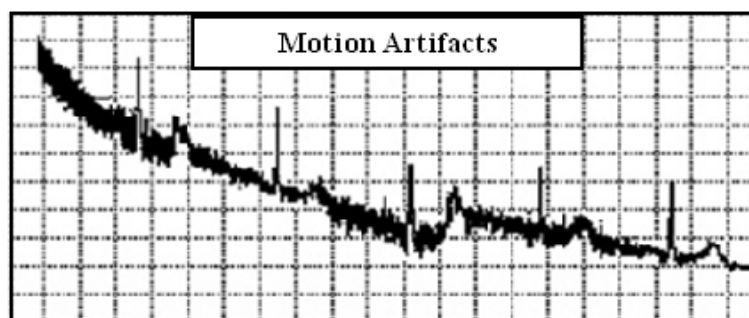


Fig. 1.6 Motion artifacts in ECG signal [6].

1.5.4 Muscle contraction (EMG)

Generally muscle contraction is produced due to muscle electrical activity. The signals resulting from muscle contraction is assumed to be transient bursts of zero-mean band-limited Gaussian noise [9]. Electromyogram (EMG) interferences generate rapid fluctuation which is very faster than ECG wave. Its frequency content is dc to 10 KHz and duration is 50 ms [9]. To remove the interference of due to EMG a morphological filter of a unit square-wave structuring (best width is 0.07 s) is used [7].

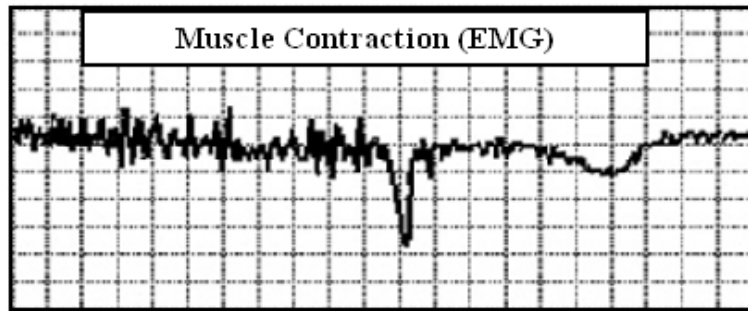


Fig. 1.7 Muscle contraction.

1.6 Arrhythmias in ECG signal

The normal rhythm of the heart where there is no disease or disorder in the morphology of ECG signal is called Normal sinus rhythm (NSR). The heart rate of NSR is generally characterized by 60 to 100 beats per minute. The regularity of the R-R interval varies slightly with the breathing cycle.

When the heart rate increases above 100 beats per minute, the rhythm is known as sinus tachycardia. This is not an arrhythmia but a normal response of the heart which demand for higher blood circulation [1]. If the heart rate is too slow then this is known as bradycardia and this can adversely affect vital organs. When the heart rate is too fast, the ventricles are not completely filled before contraction for which pumping efficiency drops, adversely affecting perfusion.

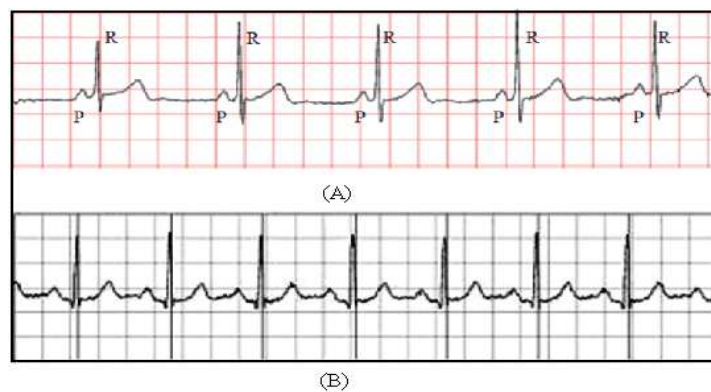


Fig. 1.8 (A) Normal sinus rhythm, (B) Sinus tachycardia

Arrhythmias are may be categories in the following manner:

1.6.1 Sinus Node Arrhythmias

This type of arrhythmia arises from the S-A node of heart. As the electrical impulse is generated from the normal pacemaker, the characteristic feature of these arrhythmias is that P-wave morphology of the ECG is normal. These arrhythmias are the following types: Sinus arrhythmia, Sinus bradycardia, and Sinus arrest etc.

1.6.2 Atrial Arrhythmias

Atrial arrhythmias originate outside the S-A node but within the atria in the form of electrical impulses. These arrhythmias types are given bellow,

Premature Atrial Contractions (PAC)

This arrhythmias results an abnormal P-wave morphology followed by a normal QRS-complex and a T-wave. This happens because of an ectopic pacemaker firing before the S-A node. PACs may occur as a couplet where two PACs are generated consecutively. When three or more consecutive PACs occur, the rhythm is considered to be atrial tachycardia.

Atrial Tachycardia

The heart rate atrial tachycardia is fast and ranges from 160 to 240 beats per minute in atrial tachycardia. Frequently atrial tachycardia is accompanied by feelings of palpitations, nervousness, or anxiety.

Atrial Flutter

In atrial flutter, the atrial rate is very fast, ranging from 240 to 360 per minute. The abnormal P-waves occur regularly and so quickly that they take morphology of saw-tooth waveform which is called flutter (F) waves.

Atrial Fibrillation

The atrial rate exceeds 350 beats per minute in this type of arrhythmias. This arrhythmia occurs because of uncoordinated activation and contraction of different parts of the atria. The higher atria rate and uncoordinated contraction leads to ineffective pumping of blood into the ventricles. Atrial fibrillation may be intermittent, occurring in paroxysms (short bursts) or chronic [1].



Fig. 1.9 Atrial arrhythmias, (A) Premature Atrial Contractions, (B) atrial tachycardia, (C) Atrial Flutter, (D) atrial fibrillation

1.6.3 Junctional Arrhythmias

Junctional arrhythmias are originated within the A-V junction in the form of the impulse comprising the A-V node and it's Bundle. The abnormal in P wave morphology occurs because of this arrhythmias [1]. The polarity of the abnormal P-wave would be opposite to that of the normal sinus P-wave since depolarisation is propagated in the opposite direction – from the A-V node towards the atria.

Premature Junctional Contractions (PJC)

It is a ventricular contraction initiated by an ectopic pacemaker in the atrioventricular (A-V) node. In premature junctional escape contraction, a normal-looking QRS complex prematurely appears, but without a preceding P-wave, but the morphology of T-wave is normal [1].

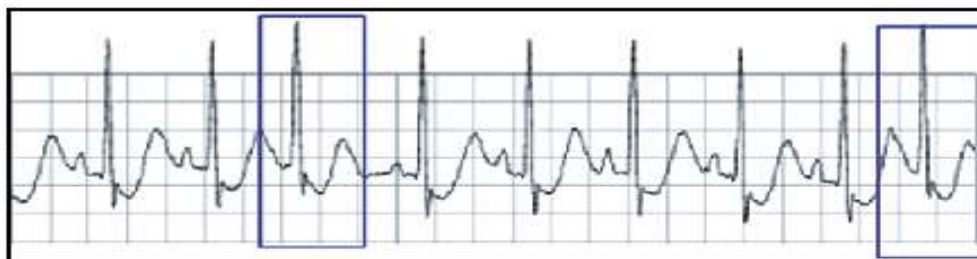


Fig. 1.10 Junctional arrhythmias.

1.6.4 Ventricular arrhythmias

In this type of arrhythmias, the impulses originate from the ventricles and move outwards to the rest of the heart. In Ventricular arrhythmias, the QRS-complex is wide and bizarre in shape.

Premature Ventricular Contractions (PVC)

In PVC the abnormality is originated from ventricles. PVCs usually do not depolarise the atria or the S-A node and hence the morphology of P-waves maintain their underlying rhythm and occur at the expected time. PVCs may occur anywhere in the heart beat cycle. PVCs are described as isolated if they occur singly, and as couplets if two consecutive PVCs occur.

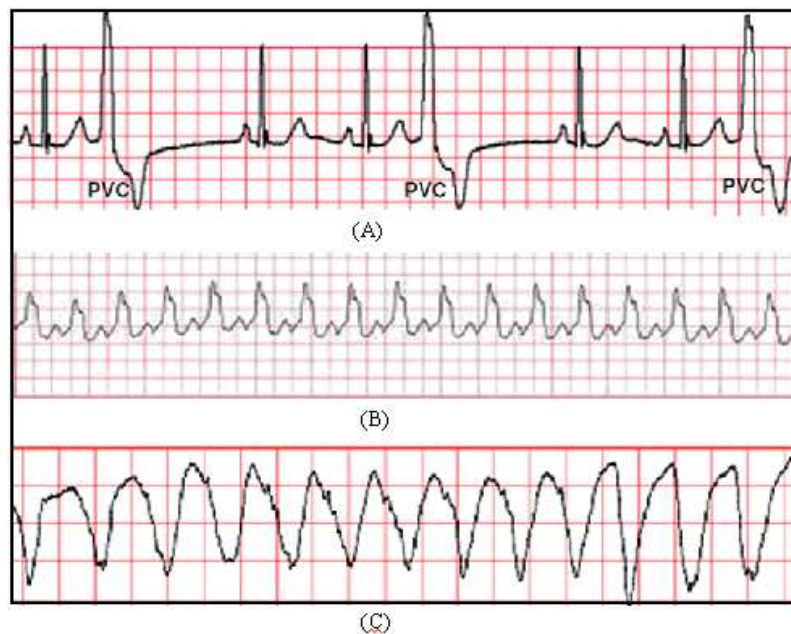


Fig. 1.11 Junctional arrhythmias (A) Premature Ventricular Contractions, (B) Ventricular Tachycardia, (C) Ventricular Fibrillation [1].

Ventricular Tachycardia (VT)

The heart rate of ventricular tachycardia is 110 to 250 beats per minute. In VT the QRS complex is abnormally wide, out of the ordinary in shape, and of a different direction from the normal QRS complex. VT is considered life-threatening as the rapid rate may prevent effective ventricular filling and result in a drop in cardiac output.

Ventricular Fibrillation

Ventricular fibrillation occurs when numerous ectopic pacemakers in the ventricles cause different parts of the myocardium to contract at different times in a non-synchronised fashion. Ventricular flutter exhibits a very rapid ventricular rate with a saw-tooth like ECG waveform.

1.6.5 Atrioventricular Blocks

It is the normal propagation of the electrical impulse along the conduction pathways to the ventricles, but the block may delay or completely prevent propagation of the impulse to the rest of the conduction system.

A first-degree AV block is occurred when all the P-waves are conducted to the ventricles, but the PR-interval is prolonged. Second-degree AV blocks are occurred when some of the P-waves fail to conduct to the ventricles. In third-degree AV block, the rhythm of the P-waves is completely dissociated from the rhythm of the QRS-complexes. Each beat at their own rate [1].

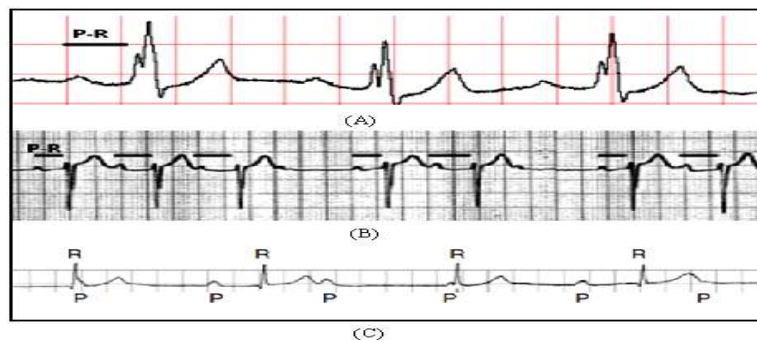


Fig. 0.12 Atrioventricular Blocks (A) first degree AV block, (B) Second degree AV block, (C) Third degree AV blocks.

1.6.6 Bundle Branch blocks

Bundle branch block, cease in the conduction of the impulse from the AV-node to the whole conduction system. Due to this block there may occur myocardial infarction or cardiac surgery [1].



Fig. 1.13 Bundle Branch blocks.

The bundle branch block beat is categorized into two types. These are Left bundle branch block beat (LBBB) and Right bundle branch block beat (RBBB). In LBBB the left bundle branch will prevent the electrical impulses from the A-V node from depolarising the left ventricular myocardium in the normal way. When the right bundle branch is blocked, the electrical impulse from the AV node is not able to propagate to the conduction network to depolarise the right ventricular myocardium.

1.7 ECG Database

1.7.1 MIT-BIH Arrhythmias database

The MIT/BIH arrhythmia database [10] is used in the study for performance evaluation. The database contains 48 records, each containing two-channel ECG signals for 30 min duration selected from 24-hr recordings of 47 individuals. There are 116,137 numbers of QRS complexes in the database [11]. The subjects were taken from, 25 men aged 32 to 89 years, and 22 women aged 23 to 89 years and the records 201 and 202 came from the same male subject. Each recording includes two leads; the modified limb lead II and one of the modified leads V1, V2, V4 or V5. Continuous ECG signals are band pass-filtered at 0.1–100 Hz and then digitized at 360 Hz. Twenty-three of the recordings (numbered in the range of 100–124) are intended to serve as a representative sample of routine clinical recordings and 25 recordings (numbered in the range of 200–234) contain complex ventricular, junctional, and supraventricular arrhythmias. The database contains annotation for both timing information and beat class information verified by independent experts [12].

1.7.2 AAMI Standard

MIT-BIH heartbeat types are combined according to Association for the Advancement of Medical Instrumentation (AAMI) recommendation [13]. AAMI standard emphasizes the problem of classifying ventricular ectopic beats (VEBs) from the non-ventricular ectopic beats [14]. AAMI also recommends that each ECG beat can be classified into the following five heartbeat types [15]:

- i. N (Normal beat)
- ii. S (supraventricular ectopic beats (SVEBs))
- iii. V (ventricular ectopic beats (VEBs))

- iv. F(fusion beats)
- v. Q (unclassifiable beats)

Each class includes heartbeats of one or more types as shown in Table 1.2. Class N contains normal and bundle branch block beat types and escape beat, class S contains supraventricular ectopic beats (SVEBs), class V contain Premature ventricular contraction beats and ventricular escape beat, class F contains beats that result from fusing normal and VEBs, and class Q contains unknown beats including paced beats.

Table 1.3 Mapping the MIT-BIH arrhythmia database heartbeat types to the AAMI heartbeat classes [15]

AAMI beat class description	Normal beat (N)	Supraventricular ectopic beat (S)	ventricular ectopic beat(V)	Fusion beat (F)	Unknown beat (Q)
MIT-BIH heart beat types	Normal beat (N)	Atrial premature beat (A)	Premature ventricular contraction (V)	Fusion of ventricular and normal beat (F)	Paced beat (/)
	Left bundle branch block beat (L)	Aberrated atrial premature beat (a)	ventricular escape beat (E)		Fusion of paced and normal beat (f)
	Right bundle branch block beat (R)	Nodal (junctional) premature beat (J)			Unclassified beat (Q)
	Atrial escape beat (e)	Supraventricular premature beat (S)			
	Nodal (junctional) escape beat (j)				

1.8 Motivation

The state of cardiac heart is generally reflected in the shape of ECG waveform and heart rate. ECG, if properly analyzed, can provide information regarding various diseases related to heart. However, ECG being a non-stationary signal, the irregularities may not be periodic and may not show up all the time, but would manifest at certain irregular intervals during the day. Clinical observation of ECG can hence take long hours and can be very tedious. Moreover, visual analysis cannot be relied upon and the possibility of the analyst missing the vital information is high. Hence, computer based analysis and classification of diseases can be very helpful in

diagnosis. Various contributions have been made in literature regarding beat detection and classification of ECG signal. Most of them use either time or frequency domain representation of the ECG waveforms, on the basis of which many specific features are defined, allowing the recognition between the beats belonging to different classes. The most difficult problem faced by today's automatic ECG analysis is the large variation in the morphologies of ECG waveforms. Moreover, we have to consider the time constraints as well. Thus our basic objective is to come up with a simple method having less computational time without compromising with the efficiency. This objective has motivated me to search and experiment with various techniques. In this thesis, R-peak detection of ECG signal is implemented using the properties of autocorrelation and Hilbert transform and classification has been done using multilayer perceptron (MLP) and radial basis function (RBF), taking the features as temporal features, heart beat interval features and ECG morphological features.

1.9 Thesis Outline

The Chapter 1 of the thesis explains the basic of ECG and ECG morphology. Different modes of lead placement and the MIT-BIH arrhythmias database are discussed. This chapter also explains the different types of arrhythmias in ECG signal.

In Chapter 2 a new method is developed using autocorrelation and Hilbert transform for detection of QRS complex in ECG signal which is the first step of ECG signal analysis.

The various characteristics features of ECG are extracted, which contains both temporal and morphological features of each heart beat. In Chapter 3 feature extraction methodology of above features are discussed.

ECG arrhythmias beat classification using multilayer perceptron (MLP) neural network and Radial basis function neural network (RBF) are discussed in Chapter 4

Chapter 5 gives the conclusion and future work of the thesis.

References

- [1] R. Acharya, J. S. Suri, J. A.E. Spaan and S .M. Krishnan, *Advances in Cardiac Signal Processing*, springer, pp. 1-50.
- [2] W. J. Germann and C. L. Standfield, "Principles of Human Physiology," Benjamin Cummings, San Francisco, 2002.

- [3] A. J. Moss and S. Stern., “Noninvasive Electro cardiology,” Clinical Aspects of Holter, London, Philadelphia, W.B. Saunders, 1996.
- [4] M. Gabriel Khan, “Rapid ECG interpretation” Third edition, 2003.
- [5] Francis Morris, June Edhouse, William J Brady, John Camm, “ABC of Clinical Electrocardiography,” BMJ Books, 2003.
- [6] <http://en.wikipedia.org/wiki/Electrocardiography>.
- [7] Y.C. Yeha, and W. J. Wang, “QRS complexes detection for ECG signal The Difference Operation Method (DOM),” *Computer methods and programs in biomedicine*, vol. 9, pp. 245–254, 2008.
- [8] R.M. Rangayyan, *Biomedical Signal Analysis: A Case-study Approach*, Wiley–Interscience, New York, pp. 18–28, 2001.
- [9] G.M. Friesen, T.C. Jannett, M.A. Jadallah, S.L. Yates, S.R. Quint, and H.T. Nagle, “A comparison of the noise sensitivity of nine QRS detection algorithm,” *IEEE Trans. Biomed. Eng.* Vol. 37, pp. 85–98, 1990.
- [10] MIT-BIH Database distribution, Massachusetts Institute of Technology, 77 Massachusetts Avenue, Cambridge, MA 02139, 1998. <http://www.physionet.org/physiobank/database/mitdb/>
- [11] B.U. Kohler, C. Henning, and R. Orglmeister, “The principles of software QRS detection,” *IEEE Eng. Med. Biol.* Vol. 21, pp. 42–57, 2002.
- [12] T. Ince, S. Kiranyaz, and M. Gabbouj, “A generic and robust system for automated patient-specific classification of ECG signals,” *IEEE Trans. Biomed. Eng.* vol. 56, pp. 1415–1426, 2009.
- [13] American National Standard for Ambulatory Electrocardiographs, publication ANSI/AAMI EC38-1994, Association for the Advancement of Medical Instrumentation, 1994.
- [14] Omern T. Inan, L. Giovangrandi, and T. A. Kovacs, “Robust Neural network based classification of Premature Ventricular Contraction using wavelet transform and time interval features,” *IEEE Trans. Biomed. Eng.* vol. 53, pp. 2507–2515, 2006.
- [15] P.de Chazal, M.O. Duyer, and R.B. Reilly, “Automatic classification of heartbeat using ECG morphology and heart beat interval features,” *IEEE Trans. Biomed. Eng.* vol. 51, pp. 1196–1206, 2004.

CHAPTER 2

QRS Complex Detection

2.1 Introduction

The detection of QRS complex is the first step towards automated computer-based ECG signal analysis. To detect the QRS complex more accurately it is necessary to identify the exact R-peak location from the recorded data. Morphological differences in the ECG waveform increase the complexity of QRS detection, due to the high degree of heterogeneity in the QRS waveform and the difficulty in differentiating the QRS complex from tall peaked P or T waves [1].

Several techniques are reported to improve the accuracy of QRS complex detection from ECG signal because the exact detection of QRS complex is difficult, as the ECG signal is added with different types of noise like electrode motion, power-line interferences, baseline wander, muscles noise etc. [2]. Pan and Tompkins [3] reported a technique where, the detection of QRS complex was achieved by linear filtering, non-linear transformation and decision rule algorithm. In another method [4] the QRS complex of ECG signal was found out using multi rate signal processing and filter banks. As reported in [3] the QRS complex can be found after finding the R-peak by differential operation in ECG signal. The first differentiation of ECG signal and its Hilbert transform is used to find the location of R-peak in the ECG signal [5].

2.2 Hilbert transform

The Hilbert transform of a real function $k(t)$ is defined as

$$\hat{k}(t) = H[k(t)] = \frac{1}{\pi} \int_{-\infty}^{+\infty} k(\tau) \frac{1}{t-\tau} d\tau = k(t) * \frac{1}{\pi t} \quad (2.1)$$

The Hilbert Transform can be interpreted from this relation as a convolution between $k(t)$ and $\frac{1}{\pi t}$. Applying the Fourier transforms to the equ.2.1, we have

$$F\{\hat{k}(t)\} = \frac{1}{\pi} F\left\{\frac{1}{t}\right\} F\{k(t)\} \quad (2.2)$$

Since,

$$F\left\{\frac{1}{t}\right\} = \int_{-\infty}^{+\infty} \frac{1}{k} e^{-j2\pi f k} dk = -j\pi \operatorname{sgn} f \quad (2.3)$$

Where

$$\text{sgn } f = \begin{cases} +1; & f > 0 \\ 0; & f = 0 \\ -1; & f < 0 \end{cases}$$

then the Fourier transform of (2.2) can be written as

$$F \{ \hat{k}(t) \} = -j \text{sgn } f F \{ k(t) \} \quad (2.4)$$

In the frequency domain, the result is then obtained by multiplying the spectrum of the $k(t)$ by j (+90) for negative frequencies and $-j$ (-90) for positive frequencies. The time domain result can be obtained after performing an inverse Fourier transform. The Hilbert transform of the original function represents its harmonic conjugate.

The pre-envelope of a real signal can be described by the expression:

$$e(t) = k(t) + j\hat{k}(t) \quad (2.5)$$

Where, $k(t)$ = real value signal

$\hat{k}(t)$ = complex value function which is the Hilbert transforms pair of $k(t)$

The envelope $E(t)$ of $e(t)$ is defined by

$$E(t) = \sqrt{k^2(t) + \hat{k}^2(t)} \quad (2.6)$$

The envelope determined using (2.6) will have the same slope and magnitude of the original signal $k(t)$ at or near its local maxima. From (2.6) it can be observed that $E(t)$ is always a positive function. Hence the maximum contribution to $E(t)$ at points where $k(t)=0$ is given by the Hilbert transform.

2.3 Methodology

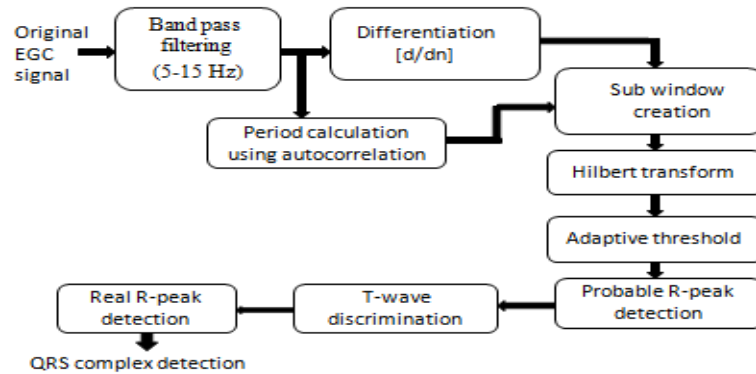


Fig. 2.1 Block diagram representation of the proposed method for detection of QRS complex.

A new approach to QRS detection using the Hilbert transform and autocorrelation function is proposed. The block diagram of the proposed method is shown in the fig.2.1. The detail description of the proposed method is given bellow

2.3.1 Filtering

The main function of the stage is to increase the signal to noise ratio of ECG signal by emphasizing the QRS complex. A band pass FIR Butterworth filter of pass band frequencies of 5-15 Hz is used to remove the power-line interference and high frequency noises from the original signal. The approximate popular pass band to maximize the QRS energy is 5-15Hz [3].

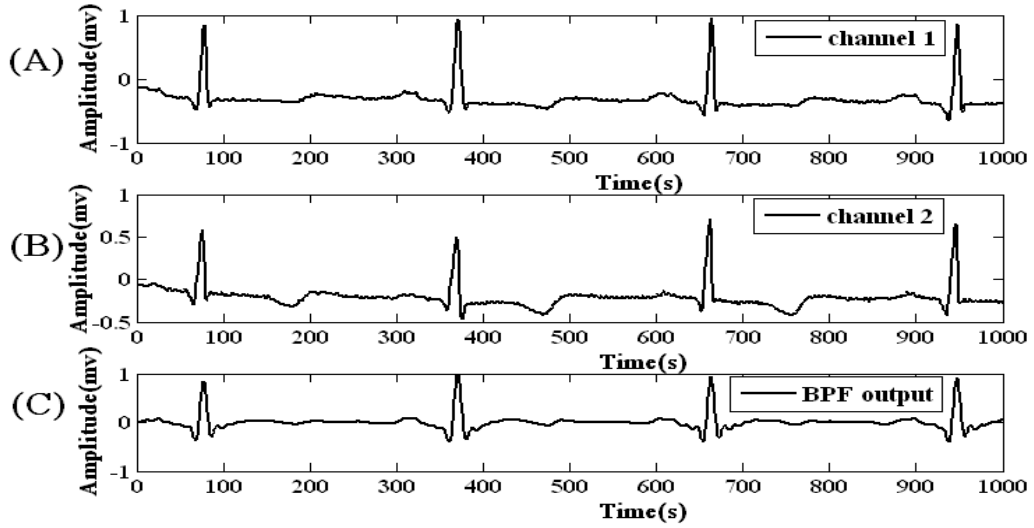


Fig. 2.2 ECG signal in the database MIT-BIH tape #100 in the range (0-1000) samples. (a) channel-1output, (b) channel-2output, (c) band pass filter output.

2.3.2 Differentiation

The first order differentiation of filtered ECG signal is taken to remove motion artifacts and baseline drifts [18]. The main function of first order differentiation is to indicate high slope points which show that the rising of signal from Q to R is the maximum slope and the falling of signal from R to S is the minimum slope of ECG signal. Therefore R peak is the zero crossing between these two positive and negative peaks, which is shown in fig.2.3.

The first differential of the given ECG signal in discrete domain can be obtained by,

$$z(n) = \frac{1}{2\Delta t} [k(n+1) - k(n-1)] \quad (2.7)$$

where, $n= 2, 3 \dots , m-1$

m is the total number of samples and Δt is the sampling time.

The first order differentiation given by (2.7) shifts the sample by one unit.

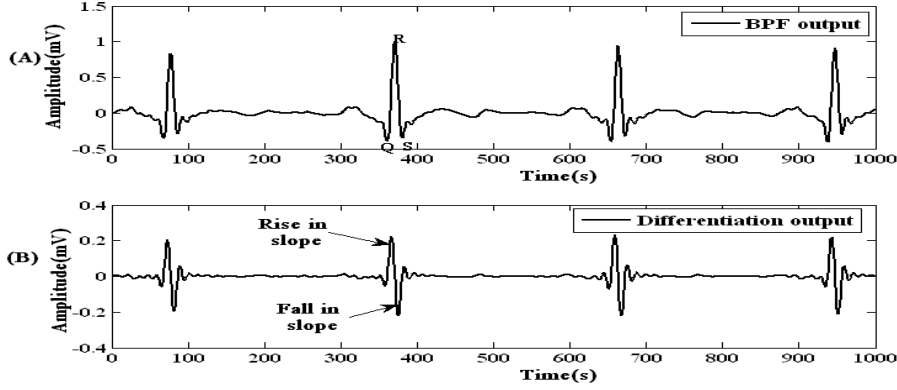


Fig. 2.3 Sample beats from ECG signal of tape #100 in MIT-BIH database (a) band pass filter output, (b) derivative output.

2.3.4 Period calculation using autocorrelation

In the proposed method 3s duration of ECG signal is extracted from the filtered ECG signal to find the exact duration of one cardiac cycle in that particular ECG signal. The approximate R-R interval between two cardiac cycles is 0.4s to 1.2s [4], [7]. So an array lag_sec is created by taking a fixed length signal of 3s duration whose sampling frequency (f_s) =360 Hz. The array length is lies in between the range 0.4s to 1.2s with a time lag 0.02s. The number of samples corresponding to each lag_sec is found out by multiplying the sampling frequency (f_s) and store these values in an array lag_index as illustrated in (2.8).

$$lag_index(i) = floor(lag_sec(i) * f_s) \quad (2.8)$$

Then the autocorrelation of ECG signal is determined by the algorithm-1

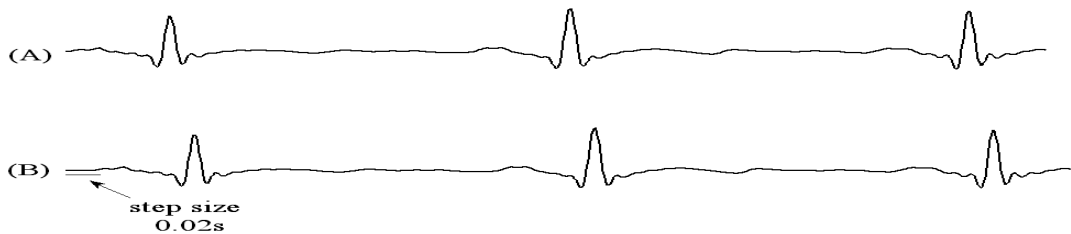


Fig. 2.4 (a) filtered signal in the database MIT-BIH tape #100 in range 0-3s, (b) shifted version of above signal with a time lag (step size) of 0.02s.

Algorithm-1: Period calculation of one cardiac cycle in ECG signal using autocorrelation
<ol style="list-style-type: none"> 1. Take an ECG signal of length 3s and denote it as $X(t)$ 2. Assign an array lag_sec in the range 0.4s to 1.2s with step size 0.02s 3. $lag_index = lag_sec * f_s$; 4. Find autocorrelation For $j=1:length(lag_index)$ do: For $i=1:(length(X)-lag_index(j))$ do: $sum(j)=sum(j)+abs(X(i))*abs(X(i+lag_index(j)))$; End for. $sum(j)=sum(j)/((length(X))-(lag_index(j)))$; End for. 5. The position where the sum is maximum indicate the period of one cardiac cycle

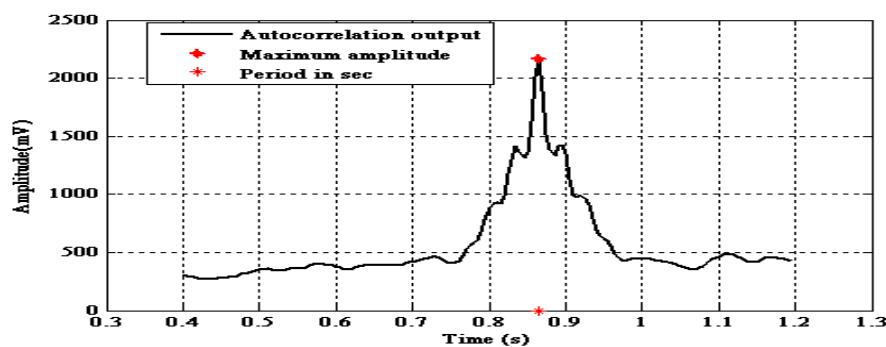


Fig. 2.5 Autocorrelation output between the signals of fig. 2.4. (a) and (b). The maximum amplitude shows where two signals are correlated. The position where amplitude is maximum shows the period of one cardiac cycle.

2.3.5 Sub window creation

The filtered ECG signal is divided into several sub-windows whose length equal to the one cardiac cycle duration. The one cardiac cycle duration is obtained from the section 2.3.3. The sub window creation helps to calculate the exact number of R-peak and its position.

2.3.6 High slope point detection using Hilbert transform

For the time varying analytic signal the Hilbert transform is used for envelope detection. The maximum peak in the envelope of Hilbert transform output is the zero crossing point of differentiation output as shown in fig. 2.6. The zero crossing point of differentiation output is the

R-peak point in the QRS complex of ECG signal [18]. The Hilbert transform of one cardiac cycle duration length signal is calculated. The maximum value of the signal after taking HT in a particular window represents the probable R-peak. Thus it shows that these peaks are not the real peaks and these peaks differ from the true R-peak position by a few milliseconds.

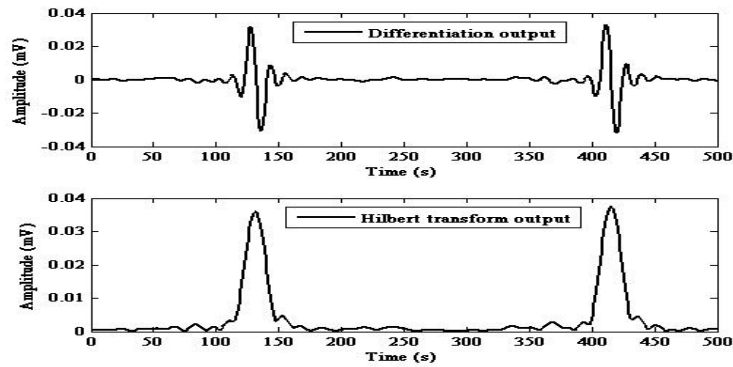


Fig. 2.6 The maximum peak of Hilbert transform output is the zero crossing of differentiation output.

2.3.7 Adaptive threshold for noise removing

The adaptive threshold technique is used to remove the noise level from the output of HT, which is describing the algorithm-2.

Algorithm-2: Adaptive threshold technique for removing noise in HT output
<ol style="list-style-type: none"> 1. Find equivalent RMS value of HT output 2. Find number of window and assign it with variable index w 3. Find maximum amplitude in a particular window and assign it as variable index \max 4. For $i=1$:no. of window do: 5. If($RMS(i) > 0.18 * \max(i)$) then do: <ul style="list-style-type: none"> If($(RMS(i) > \max(i)) \& \& (RMS(i) < \max(i-1))$) then do: <ul style="list-style-type: none"> $Thr(i) = 0.39 * \max(i)$; Else If($(RMS(i) > \max(i)) \& \& (RMS(i) > \max(i-1))$) <ul style="list-style-type: none"> $Thr(i) = 0.39 * \max(i-1)$; End if. 6. Else If($RMS(i) < 0.18 * \max(i)$) then do: <ul style="list-style-type: none"> $Thr(i) = 1.6 * RMS(i)$; End if.

2.3.8 T wave discrimination

After finding the probable R-peaks search back technique is used to discriminate the T wave. The maximum amplitude within a 200ms window length is set to find the real R-peaks from probable R-peaks.

2.3.9 Second stage detector to find Q and S point

A second stage detector is used to locate the Q & S point in ECG. A window containing ± 10 sample from the location of the R-peak is selected in the original ECG waveform to locate these points.

2.4 Result and discussion

In order to evaluate the performance, the proposed algorithm was tested using MIT-BIH Arrhythmia database [8]. The algorithm is able to detect the QRS complex more accurately as shown in the Fig.7. The total performance is shown in the form of tabulation in Table 2.1.

The performance is analyzed using the following parameters

1. Sensitivity (Se): This indicates the percentage of true beats that were correctly detected by the algorithm.

$$\text{Sensitivity}(\%) = \frac{TP}{TP + FN} \quad (2.8)$$

1. Positive Predictivity (+p): It gives the percentage of heart beat detection which are reality true beats.

$$\text{Positive predictive}(\%) = \frac{TP}{TP + FP} \quad (2.9)$$

2. Detection error rate (%):

$$\text{Detection error rate}(\%) = \frac{FP + FN}{\text{Total number of QRS complex}} \quad (2.10)$$

Where, TP=Number of true positive beat detected

FP= Number of false positive beat

FN= Number of false negative beat

TN=Number of true negative beat

Table 2.1 The result of the proposed method for the signals in MIT-BIH database

MIT-BIH records	True Positive Beat (TP)	False Positive Beat (FP)	False Negative Beat (FN)	Failed detection (FP+FN)	Sensitivity (Se)	Positive predictivity (%)	Detection error rate (%)
100	2273	0	0	0	100.00	100.00	0.00
101	1865	2	1	3	99.95	99.89	0.16
102	2187	3	1	4	99.95	99.86	0.18
103	2084	0	0	0	100.00	100.00	0.00
104	2230	2	1	3	99.96	99.91	0.13
105	2572	3	7	10	99.73	99.88	0.39
106	2027	2	2	4	99.90	99.90	0.20
107	2137	2	4	6	99.81	99.91	0.28
108	1763	6	0	6	100.00	99.66	0.34
109	2532	2	3	5	99.88	99.92	0.20
111	2124	0	1	1	99.95	100.00	0.05
112	2539	0	0	0	100.00	100.00	0.00
113	1795	0	0	0	100.00	100.00	0.00
114	1879	2	1	3	99.95	99.89	0.16
115	1953	0	0	0	100.00	100.00	0.00
116	2412	5	1	6	99.96	99.79	0.25
117	1535	0	1	1	99.93	100.00	0.07
118	2275	0	1	1	99.96	100.00	0.04
119	1987	1	0	1	100.00	99.95	0.05
121	1863	0	1	1	99.95	100.00	0.05
122	2476	0	0	0	100.00	100.00	0.00
123	1518	0	0	0	100.00	100.00	0.00
124	1619	0	0	0	100.00	100.00	0.00
200	2607	0	1	1	99.96	100.00	0.04
201	1963	0	4	4	99.80	100.00	0.20
202	2136	0	5	5	99.77	100.00	0.23
203	2982	0	2	2	99.93	100.00	0.07
205	2656	4	2	6	99.92	99.85	0.23
207	1862	0	2	2	99.89	100.00	0.11
208	2956	3	2	5	99.93	99.90	0.17
209	3004	0	0	0	100.00	100.00	0.00
210	2647	1	3	4	99.89	99.96	0.15
212	2748	0	0	0	100.00	100.00	0.00
213	3251	1	6	7	99.82	99.97	0.22
214	2262	3	1	4	99.96	99.87	0.18
215	3363	2	0	2	100.00	99.94	0.06
217	2208	1	3	4	99.86	99.95	0.18
219	2154	2	0	2	100.00	99.91	0.09
220	2048	0	1	1	99.95	100.00	0.05
221	2427	0	5	5	99.79	100.00	0.21
222	2484	2	5	7	99.80	99.92	0.28
223	2605	0	4	4	99.85	100.00	0.15
228	2053	0	3	3	99.85	100.00	0.15
230	2256	3	0	3	100.00	99.87	0.13
231	1186	2	0	2	100.00	99.83	0.17
232	1780	1	4	5	99.78	99.94	0.28
233	3079	0	5	5	99.84	100.00	0.16
234	2735	0	0	0	100.00	100.00	0.00
48 patients	116,137	55	83	138	99.93	99.95	0.12

Table 2.2 The comparison of the proposed method with the Pan-Tompkins (PT) method and difference operation method (DOM).

Tape #	Total beats	PT method			DOM method			Proposed method		
		FP	FN	Failed detection %	FP	FN	Failed detection %	FP	FN	Failed detection %
100	2273	0	0	0.00	0	1	0.04	0	0	0.00
101	1865	5	3	0.43	0	1	0.05	2	1	0.16
102	2187	0	0	0.00	0	1	0.05	3	1	0.18
103	2084	0	0	0.00	0	0	0.00	0	0	0.00
104	2230	1	0	0.04	2	0	0.09	2	1	0.13
105	2572	67	22	3.46	0	17	0.66	3	7	0.39
106	2027	5	2	0.35	0	6	0.30	2	2	0.20
107	2137	0	2	0.09	0	3	0.14	2	4	0.28
108	1763	199	22	12.54	6	0	0.34	6	0	0.34
109	2532	0	1	0.04	0	3	0.12	2	3	0.20
111	2124	1	0	0.05	0	1	0.05	0	1	0.05
112	2539	0	1	0.04	1	0	0.04	0	0	0.00
113	1795	0	0	0.00	9	0	0.50	0	0	0.00
114	1879	3	17	1.06	0	1	0.05	2	1	0.16
115	1953	0	0	0.00	0	0	0.00	0	0	0.00
116	2412	3	22	1.04	0	17	0.70	5	1	0.25
117	1535	1	1	0.13	2	0	0.13	0	1	0.07
118	2275	1	0	0.04	10	0	0.44	0	1	0.04
119	1987	1	0	0.05	0	0	0.00	1	0	0.05
121	1863	4	7	0.59	0	2	0.11	0	1	0.05
122	2476	1	1	0.08	0	0	0.00	0	0	0.00
123	1518	0	0	0.00	0	0	0.00	0	0	0.00
124	1619	0	0	0.00	1	0	0.06	0	0	0.00
200	2607	6	3	0.35	5	0	0.19	0	1	0.04
201	1963	0	10	0.51	0	20	1.02	0	4	0.20
202	2136	0	4	0.19	1	0	0.05	0	5	0.23
203	2982	53	30	2.78	16	2	0.60	0	2	0.07
205	2656	0	2	0.08	0	16	0.60	4	2	0.23
207	1862	4	4	0.43	0	1	0.05	0	2	0.11
208	2956	4	14	0.60	0	14	0.47	3	2	0.17
209	3004	3	0	0.10	1	0	0.03	0	0	0.00
210	2647	2	8	0.38	0	14	0.53	1	3	0.15
212	2748	0	0	0.00	1	0	0.04	0	0	0.00
213	3251	1	2	0.09	0	3	0.09	1	6	0.22
214	2262	2	4	0.26	0	4	0.18	3	1	0.18
215	3363	0	1	0.03	0	4	0.12	2	0	0.06
217	2208	4	6	0.45	0	2	0.09	1	3	0.18
219	2154	0	0	0.00	0	0	0.00	2	0	0.09
220	2048	0	0	0.00	0	0	0.00	0	1	0.05
221	2427	2	0	0.08	0	1	0.04	0	5	0.21
222	2484	101	81	7.33	0	5	0.20	2	5	0.28
223	2605	1	0	0.04	1	0	0.04	0	4	0.15
228	2053	25	5	1.46	0	2	0.10	0	3	0.15
230	2256	1	0	0.04	2	0	0.09	3	0	0.13
231	1186	0	0	0.00	0	15	0.80	2	0	0.17
232	1780	6	1	0.39	0	0	0.00	1	4	0.28
233	3079	0	1	0.03	0	9	0.29	0	5	0.16
234	2735	0	0	0.00	0	1	0.04	0	0	0.00
Total	116,137	507	277	0.68	58	166	0.19	55	83	0.12

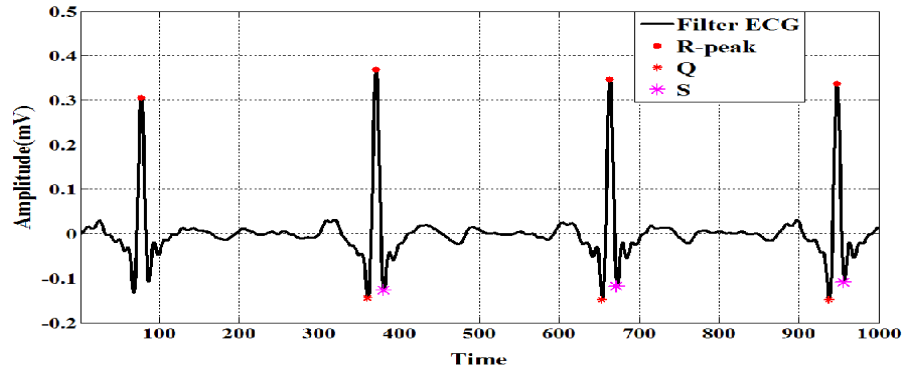


Fig. 2.7 The detected QRS point of signal tape #100

The detector achieves very good performance on the studied MIT-BIH arrhythmia database for signal with noise even in the presence of pronounced muscular noise and baseline artifacts. The QRS detector attains $Se=99.93\%$, $+P=99.95\%$, and detection error rate of 0.12% . The proposed method is compared with difference operation method and Pan-Tompkins method as shown in Table 2.2. The proposed algorithm deploying autocorrelation and Hilbert transform works better than the earlier reported technique which is based on DOM method [4] and PT method [3].

2.5 Conclusion

This chapter proposes a novel QRS detection algorithm in ECG signal, based on the properties of autocorrelation and Hilbert transform. The result of the proposed method is compared with the Pan-Tompkins (PT) method and difference operation method (DOM). In evaluating detection method for the MIT/BIH arrhythmia database, the algorithm shows the accuracy over 99.88% even in the presence of significant noise contamination. The experimental result shows that the proposed method performs better as compared to above two methods and allows a reliable and accurate detection of the QRS complexes.

References

- [1] N.V. Thakor, J.G. Webster and W.J. Tompkins , “Estimation of QRS complex power spectra for design of a QRS filter,” *IEEE Trans. Biomed. Eng.*, vol. 31, pp. 702–705, 1984.
- [2] Y.C. Yeha, and W. J. Wang, “QRS complexes detection for ECG signals The Difference Operation Method (DOM),” *Computer methods and programs in biomedicine*, vol. 9, pp. 245–254, 2008.
- [3] J. Pan, W. J. Tompkins, “A real time QRS detection algorithm,” *IEEE Trans. Biomed. Eng.*, vol. 32, pp. 230–236, 1985.

- [4] X. Afonso, W.J. Tompkins, T. Nguyen, S. Luo, "ECG beat detection using filter banks," *IEEE Trans. Biomed. Eng.*, vol. 46, pp. 230-236, 1999.
- [5] D. Benitez, P.A. Gaydeckia, A. Zaidib, and A.P. Fitzpatrick, "The use of the Hilbert transform in ECG signal analysis," *Computers in Biology and Medicine*, vol. 31, pp.399–406, 2001.
- [6] S.Ari, K. Sensharma, and G. Saha, "DSP implementation of a heart valve disorder detection system from a phonocardiogram signal," *Journal of Medical Engineering & Technology*, vol. 32, no. 2, pp.122 – 132, 2008.
- [7] R.M. Rangayyan, *Biomedical Signal Analysis: A Case-study Approach*, Wiley–Interscience, New York, pp.18-28, 2001.
- [8] MIT-BIH Database distribution, Massachusetts Institute of Technology, 77 Massachusetts Avenue, Cambridge, MA 02139,1998.<http://www.physionet.org/physiobank/database/mitdb/>
- [9] American National Standard for Ambulatory Electrocardiographs, publication ANSI/AAMI EC38-1994, Association for the Advancement of Medical Instrumentation, 1994.
- [10] N.M. Arzeno, Z. Deng and C.S. Poon, "Analysis of First –Derivative base QRS detection algorithms," *IEEE Trans. Biomed. Eng.*, vol. 55, pp. 478–484, 2008.
- [11] B.U. Kohler, C. Henning, and R. Orglmeister, "The principles of software QRS detection," *IEEE Eng. Med. Biol.* Vol. 21, pp. 42–57, 2002.
- [12] Y.H. Hu, J. Tompkins, J.L. Urrusti, and V.X. Afonso, "Application of artificial neural networks for ECG signal detection and classification," *Journal of Electrocardiology*, vol. 26, pp. 66–73, 1993.
- [13] R.J. Bolton, L.C. Westphal, "Hilbert transform processing of ECG's," 1981 *IREECON International Convention Digest*, IREE, Melbourne, pp. 281–283,1981.
- [14] Q. Xue, Y.H. Hu, W.J. Tompkins, "Neural-network-based adaptive matched filtering for QRS detection," *IEEE Trans. Biomed. Eng.* 39, pp.315–329, 1992.
- [15] Kleydis V. Suarez, Jesus C. Silva, Yannick Berthoumieu, Pedro Gomis, and Mohamed Najim, "ECG Beat Detection using a Geometrical Matching Approach," *IEEE Transactions Biomed. Engg.*, vol. 54, no. 4, 2007.
- [16] R.J. Bolton, L.C. Westphal, "On the use of the Hilbert Transform for ECG waveform processing, in: *Computers in Cardiology*," IEEE Computer Society, Silver Spring, MD, pp. 533–536, 1984.
- [17] S. G. Guillen, M. T. Arredondo, G. Martin, and J. M. F. Corral, "Ventricular fibrillation detection by autocorrelation function peak analysis," *J. Electrocardiol.*, vol. 22, pp. 253–262, 1989.

CHAPTER 3

Feature Extraction of ECG Signal

3.1 Introduction

The classification of cardiac arrhythmias can be achieved after extracting the features of each heart beat in the ECG signal. A good feature extraction methodology can accurately classify cardiac abnormalities. Several methods have been proposed for extracting features of one cardiac cycle. The features of one cardiac cycle may be time domain features or frequency domain features. In [1] Inan *et al.* found that morphological information along with timing information can provide high classification accuracy for larger dataset. The combining of wavelet domain feature with RR- interval features can achieve high classification accuracy as reported in [2]. The morphological feature along with the temporal feature of each patient specific data can give high classification accuracy [3]. Khazaei *et al.* [4] extracted power spectral density (PSD) features of each heart beat with three timing interval features classifying cardiac abnormalities in MIT-BIH database. The Hermit basis function can provide an effective approach for characterizing ECG heart beat and have been widely used in ECG signal classification [5]. As reported in [6], the authors Dutta *et al.* has proposed cross-correlation based feature for classifying PVC beats from non-PVC beats. They have used cross-correlation between each ECG heart beat signal with the normal heart beat signal which is chosen as reference signal.

In the study the time domain features of each heart beat have been extracted for classifying SVEBs and VEBs from non-SVEBs and non- VEBs followed by AAMI standard. The feature vector contains four temporal features; three heart beat interval features and nineteen fixed interval morphological features. Hence in total there are twenty six feature vectors are extracted for each heart beats which can be used for classification of cardiac arrhythmias using different classifiers. All the features are considered for single channel in the MIT-BIH arrhythmias database.

3.2 Methodology

Automatic classification ECG signal consist of different features of ECG in one cardiac cycle. Features relating to fiducial point intervals were considered for each heartbeat. Features relating to heartbeat intervals and ECG morphology were also calculated separately for each heartbeat in the ECG signals. The features are extracted for one cardiac cycle [7] as follows:

Table 3.1 Feature groups considered in this study

Group label	Features
Temporal	Pre-RR interval
	Post-RR interval
	Average RR-interval
	Local average RR-interval
Heart beat interval	QRS duration (QRS on and QRS off)
	T-Wave duration (T-Wave on and T-Wave off)
	Presence and absent of P-wave
Morphology	Normalized ECG morphology (10 sample) between QRS onset and QRS off set
	Normalized ECG morphology (9 sample) between T-Wave onset and T-Wave offset

3.2.1 RR-Interval Features

RR-interval is defined as the interval between successive heartbeat fiducial points. Four features (see Table 3.1: RR-intervals) are extracted from the RR sequence [7]. The pre-RR-interval is defined as the RR-interval between a given heartbeat and the previous heartbeat. The RR-interval between a given heartbeat and the following heartbeat is known as post-RR-interval. The average RR-interval is the mean of the RR-intervals for a recording and is considered as the same value for all heartbeats in a recording. Finally, the local average RR-interval is determined by averaging the RR-intervals of the ten RR-intervals surrounding a heartbeat.

3.2.2 Heartbeat Interval Features

Three heartbeat interval features for each single channel ECG recording (see Table 3.1: heartbeat intervals) relating to heartbeat intervals are calculated after heartbeat segmentation [7]. The time interval between the QRS onset and the QRS offset is known as QRS duration. The T-

wave duration is defined as the time period between the QRS offset and the T-wave offset. The third feature is the presence or absence of a P-wave which is indicated by a Boolean variable that means the Boolean variable '1' implies the presence of P-wave and the variable '0' shows the absence of P-wave.

3.2.3 ECG Morphology Features

Two types of ECG morphology features are taken for each heart beat (see Table 3.1: morphology). Ten features from QRS complex and nine features from T wave morphology are chosen from the selected heart beat after finding the fiducial point [7]. The above features are selected as shown in fig. 3.1. A fixed sample rate is used for extracting the morphology feature and the sampling windows are located by after detecting the heartbeat fiducial point (FP). Fig. 3.1 (b) shows the sampling process. Two sampling windows were formed based on R-peak. The window between FP-50 ms and 100 ms is considered which covers the contain of QRS-complex morphology as the portion of the ECG. A 60-Hz sampling rate is applied to the above window of the QRS-complex resulting in ten features. The second window approximately contains the T-wave morphology in between the time duration FP+150 ms and FP+500 ms. The ECG signal amplitude is sampled at 20 Hz in this window, resulting in nine features for T-wave morphology. Lower sampling rates is chosen for T-wave sampling windows as the frequency content of this wave is lower than the frequency content of the QRS-complex.

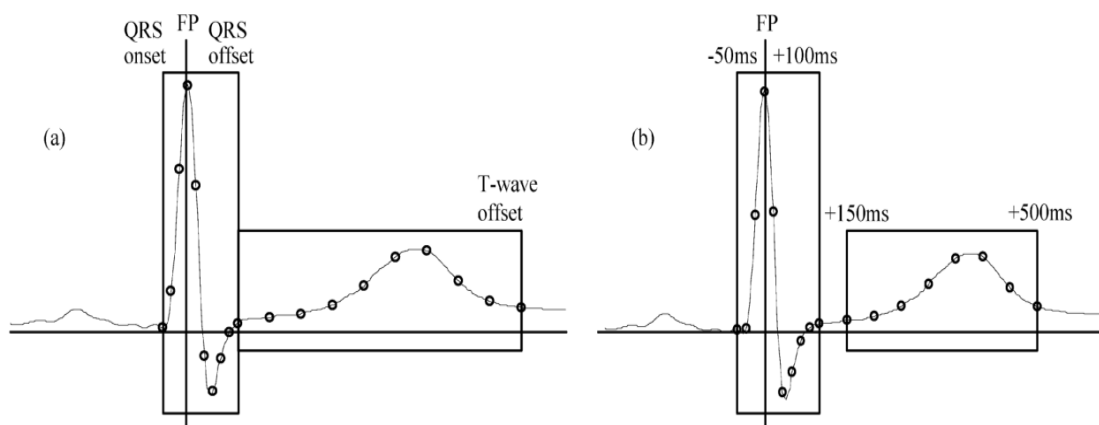


Fig. 3.1 (a) after getting fiducial point (FP), the QRS onset and offset and t-wave offset points are found, b) after determining the FP nine samples of the ECG between FP-50 ms and FP + 100 ms and nine samples between FP+150 ms and FP+500 ms are extracted [7]

3.4 Simulation result

The experimental results are found out after MATLAB simulation. The visualization results of ten QRS morphology features and nine T-wave morphology feature features of the #tape 100 in the MIT-BIH database is shown in fig.3.2. The tabulation result (see table 3.2) shows the visualization result which indicates the total number of arrhythmias present in the MIT-BIH arrhythmia database. The result implies the pictorial representation of each beat types, one cardiac feature and the corresponding twenty six feature waveform. It also indicates the #tape number as well as the beat position of which the feature is taken from the MIT-BIH arrhythmia database after reference from annotation file.

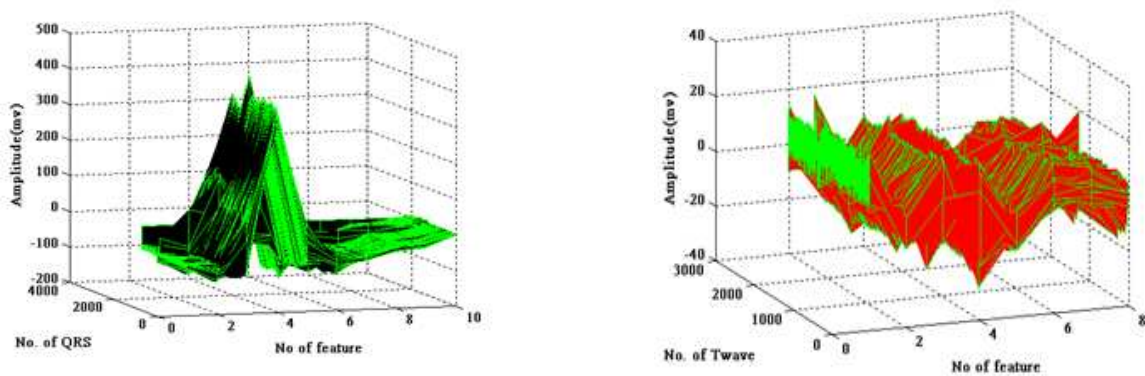
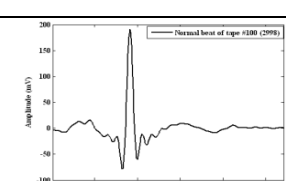
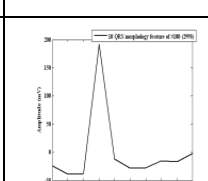
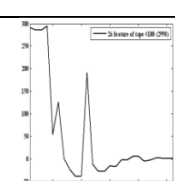
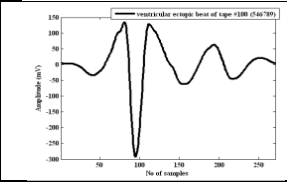
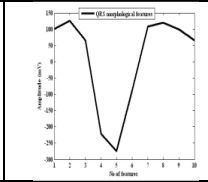
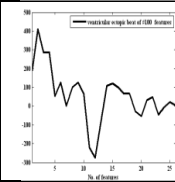
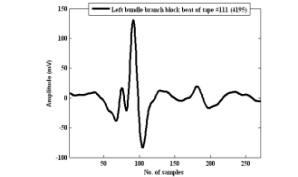
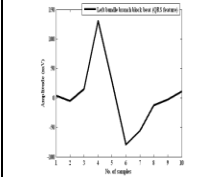
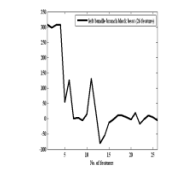
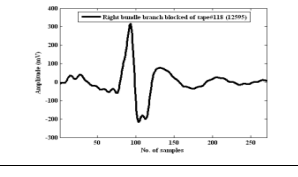
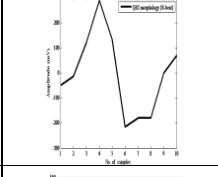
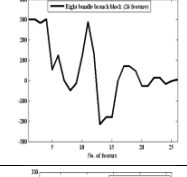
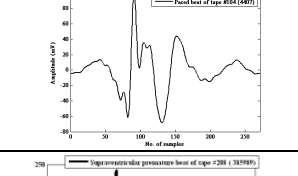
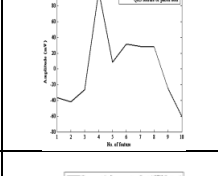
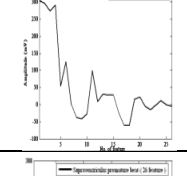
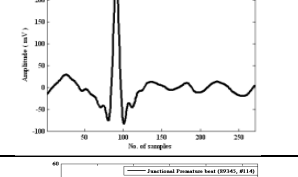
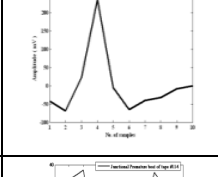
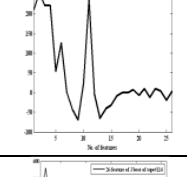
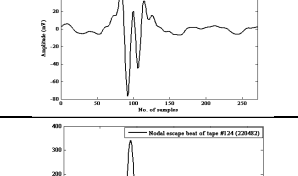
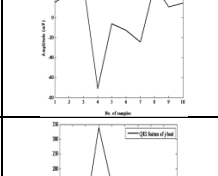
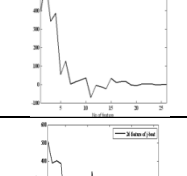
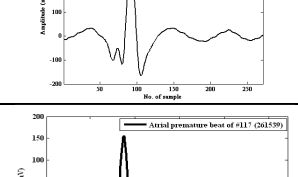
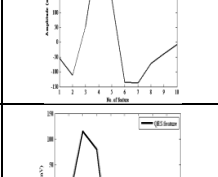
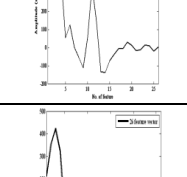
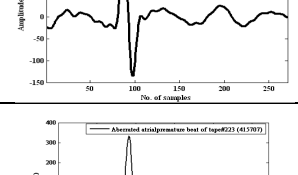
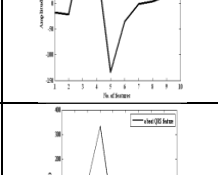
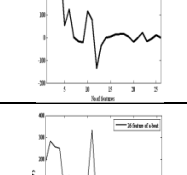
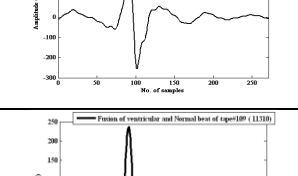
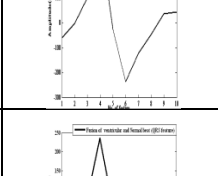
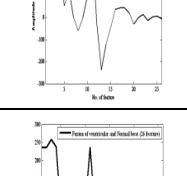
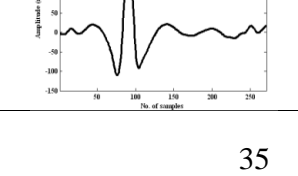
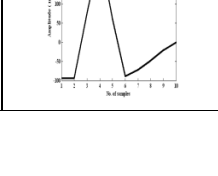
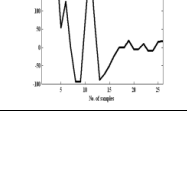


Fig. 3.2 Ten fixed interval morphology features of QRS complex (left) and nine fixed interval morphology features of T-wave (right) of tape#100 in MIT/BIH database

Table 3.2 Cardiac arrhythmia beat types in MIT/BIH database

Sl. No.	Cardiac arrhythmia type	MIT-BIH Tape No.	One cardiac Feature (271 sample)	QRS feature (10 morphological feature)	26 feature Waveform	Beat position
1	Normal beat (N)	#100				2998
2	Premature ventricular contraction beat (V)	#100				546789

3	Left bundle branch block (L)	#111				4195
4	Right bundle branch block (R)	#118				12595
5	Paced beat (I)	#104				4407
6	Supraventricular premature beat (S)	#208				385989
7	Nodal (Junctional) premature beat (J)	#114				89345
8	Nodal (Junctional) escape beat (j)	#124				220482
9	Atrial premature beat (A)	#117				261539
10	Aberrated atrial Premature beat (a)	#223				415709
11	Fusion of ventricular and normal beat (F)	#109				11310

12	Fusion of paced and normal beat (f)	#104				47033
13	Atrial escape Beat (e)	#223				43415
14	Ventricular escape beat (E)	#207				619542
15	Unclassified beat (Q)	#104				11269
16	Ventricular flutter beat (!)	207				16498

The total features are divided in to five classes according to AAMI recommendation. The table 3.3 indicates patient by patient total number of features and their corresponding class which are separated according to AAMI standard. The paced beats in the database having the #tape number 102, 104, 107 and 217 are not considered in this study as these beats are not recommended by AAMI standard. The total numbers of arrhythmia type present in the database and their comparison result with references to annotation file is given away in table 3.4. The total number of extracted features (1, 08,981) is less in comparison to annotation (1, 09,963) because of the following reasons,(i) in some #tape the T-wave features is not present at the end of the #tape which is a cardiac feature and (ii) there are some false negative beats present during the R-peak detection.

Table 3.3 Patient by patient report of each tape according to AAMI recommendation excluding the tape contains paced beat

MIT-BIH record	AAMI standard					Total
	N	S	V	F	Q	
100	2238	33	1			2272
101	1859	3			1	1863
103	2080	2				2082
105	2517		41		5	2563
106	1507		505			2012
108	1702	4	17	2		1725
109	2490		35	2		2527
111	2119		1			2120
112	2536	2				2538
113	1788	6				1794
114	1817	12	43	4		1876
115	1952					1952
116	2278	1	108			2387
117	1532	1				1533
118	2166	95	16			2277
119	1543		443			1986
121	1858	1	1			1860
122	2474					2474
123	1514		3			1517
124	1535	31	45	5		1616
total normal	39505	191	1259	13	6	40974
200	1743	30	813	1		2587
201	1633	110	198	2		1943
202	2061	48	17	1		2127
203	2512	2	409	1	1	2925
205	2569	3		10		2582
207	1540	107	207			1854
208	1586	2	961	368	2	2919
209	2621	374	1			2996
210	2379	16	144	6		2545
212	2741					2741
213	2638	28	76	347		3089
214	2003		245	1	1	2250
215	3187	3	148			3338
219	2080	7				2087
220	1953	94				2047
221	2031		374			2405
222	2268	207				2475
223	2034	68	404	14		2520
228	1680	3	360			2043
230	2255		1			2256
231	1567	1	2			1570
232	398	1381				1779
233	2222	7	809	11		3049
234	2695	50				2745
total abnormal	50396	2541	5169	762	4	58872
Total	89901	2732	6428	775	10	99846

Table 3.4 Beat summary of MIT-BIH heartbeat types

Sl. No.	Symbols	Symbol type	Annotation	Feature taken
1	N	Normal beat	75053	74846
2	L	left bundle branch block	8074	8068
3	R	Right bundle branch block	7259	7249
4	A	Atrial premature beat	2544	2525
5	a	Abberated Atrial premature beat	150	123
6	J	Nodal (Junctional) premature beat	83	83
7	S	Supraventricular premature beat	2	2
8	V	Ventricular premature beat	7129	6666
9	F	Fusion of Ventricular and normal beat	803	775
10	!	Ventricular flutter wave	472	280
11	e	Atrial escape beat	16	15
12	j	Nodal (Junctional) escape beat	229	229
13	E	ventricular escape beat	106	105
14	/	Paced beat	7028	7017
15	f	Fusion of paced and normal beat	982	971
16	Q	Unclassified beat	33	27
Total (48 tape)			109963	108981

2.5 Conclusion

The feature extraction process has been carried out after automatic detection of R-peak in ECG signal using autocorrelation and Hilbert transform method. A total of 26 feature vector for each cardiac cycle has been extracted, and is used for cardiac abnormality classification. The annotation file helps to categories the extracted feature in the respective particular classes.

References

- [1] Omern T. Inan, L. Giovangrandi, and T. A. Kovacs, "Robust Neural network based classification of Premature Ventricular Contraction using wavelet transform and time interval features," *IEEE Trans. Biomed. Eng.* vol. 53, pp. 2507-2515, 2006.

- [2] T.Ince, S. Kiranyaz, and M. Gabbouj, "A generic and robust system for automated patient-specific classification of ECG signals," *IEEE Trans. Biomed. Eng.* vol. 56, pp. 1415-1426, 2009.
- [3] P. de Chazal, R.B. Reilly, "A patient-adapting heartbeat classifier using ECG morphology and heartbeat interval feature," *IEEE Trans. Biomed. Eng.* vol. 53, pp. 2535-2543, 2006.
- [4] A. khazae, A. Ebrahimzadeh, "classification of Electrocardiogram Signal with support vector machines and genetic algorithms using power spectral features," *Biomedical signal and control*, vol. 5, pp. 252-263, 2010.
- [5] W. Jiang and S. G. Kong, "Block-based neural networks for personalized ECG signal classification," *IEEE Trans. Neural Netw.*, vol. 18, no. 6, pp. 1750-1761, Nov. 2007.
- [6] S. Dutta, A chatterjee, and S. Munchi, "Correlation technique and least square support vector machine combined for frequency domain based ECG beat classification," *Medicl Engineering & Physics*, vol. 32, pp. 1161-1169, 2010.
- [7] P.de Chazal, M.O. Duyer, and R.B. Reilly, "Automatic classification of heartbeat using ECG morphology and heart beat interval features," *IEEE Trans. Biomed. Eng.* vol. 51, pp. 1196-1206, 2004.
- [8] M.Stridh, A. Bollmann, S.B. OLSSON, and L. Sornmo, "Detection and Feature Extraction of Atrial Tachyarrhythmias," *IEEE Engg. In Medicine and Biology Magazine*, pp. 31-39, Nov. 2006.
- [9] B.A. Eisenstein, and R. J. Vaccaro, " Feature Extraction by System Identification," *IEEE Transactions on Systems, Man, And Cybernetics*, vol.-12, No. 1, 1982.
- [10] G. D. Fei, H.B. Pin and X. X. Jian, "Study of Feature Extraction Based on Autoregressive Modeling in ECG Automatic Diagnosis," *ACTA AUTOMATICA SINICA*, vol. 33, No. 5, pp. 462-466, 2007.
- [11] S. C. Saxena, V. Kumar, and S. Hamde. Feature extraction from ECG signals using wavelet transform for disease diagnostics. *IJSS*, 33:1073- 1085, 2002.
- [12] K.P. Lil and W.H. Chang, "QRS Feature Extraction Using Linear Prediction," *IEEE Trans. Biomed. Eng.* vol. 36, No. 10, 1989.
- [13] P. Laguna, R. Jané, and P. Caminal, "Automatic detection of wave boundaries in multilead ECG signals: Validation with the CSE database," *Comput. Biomed. Res.*, vol. 27, no. 1, pp. 45-60, 1994.
- [14] S. C. Saxena, A. Sharma, and S. C. Chaudhary, "*International Journal of Systems Science*," vol. 28, No. 5, pp. 483-498, 1997.

CHAPTER 4

Classification of Cardiac Arrhythmias

4.1 Introduction

Automatic ECG beat classification is essential to timely dangerous heart condition. It is a very time consuming job for doctors to analyze long ECG records. Therefore, many computer based methods have been proposed for automatically diagnosis of the ECG beat abnormalities. The main principles of such methods are based on pattern recognition techniques.

Several techniques have been proposed for cardiac arrhythmias classification. Among them the most recently published work are presented [1]-[5]. Inan *et al.* [1] presented an approach for classifying beats of a large dataset by training a neural network (NN) classifier using wavelet and timing features. Inan *et al.* found that the fourth scale of a dyadic wavelet transform with a quadratic spline wavelet together with the pre-/post RR-interval ratio is effective for distinguishing normal and premature ventricular contraction (PVC) from other beats. In [2], an approach for personalized ECG heartbeat pattern classification is presented. It is based on block-based NNs, where a 2-D array of modular component NNs with flexible structures and internal configurations is implemented using reconfigurable digital hardware. Network structure and connection weights are optimized using local gradient-based search and evolutionary operators with the rates changing adaptively according to their effectiveness in the earlier evolution period. Two classification systems based on the support vector machine (SVM) approach has been found in literature [3]. The first system exploits the features based on high-order statistics, while the second uses the coefficients of Hermite polynomials. In [4], a patient-adapting heartbeat classifier system based on linear discriminants is proposed. The system then adapts by first training a local classifier using the newly annotated beats, and combines both local and global classifiers to form an adapted classification system. In [5] Hu *et al.* combined a local classifier as well as a global classifier using a mixture of experts (MOE) approach.

The performance result of cardiac arrhythmias beat classification algorithm has been standardized by the AAMI standard [9]. The AAMI standard emphasize on classifying VEB from non-VEBs and SVEB from non- SVEBs. MIT-BIH arrhythmias [8] database has been used for performance analysis.

4.2 Multilayer perception back propagation (MLP-BP) neural network

The Multilayer Perceptron (MLP) is one of the most widely implemented neural network topologies. The basic connectionist structure has shown in fig.4.1, a feed forward NN, having single input layer, one hidden layer, and one output layer. The input layer connect the network structure to the environment and output layer give the output to the environment through output nodes. Hence the number of nodes in input layer and output layer is fixed by the problem. MLPs are normally trained with the back propagation algorithm. The back propagation rule propagates the errors through the network and allows adaptation of the hidden nodes. Two important characteristics of the multilayer perceptron are: its nonlinear processing elements (PEs) which have a nonlinearity (the logistic function, linear Tanh function and the hyperbolic tangent are the most widely used); and their massive interconnectivity (i.e. any element of a given layer feeds all the elements of the next layer). The multilayer perceptron is a supervised neural network that means the network is trained trained with the desired target response. The MLPs mainly operate with error correction learning, which means that the network output is always compared with the desired response of the system [7]. In pattern recognition this is normally the case, since we have our input and desired data labeled. Error correction learning works in the following way: From the system response at PE i at iteration n , $y_i(n)$, and the desired response $d_i(n)$ for a given input pattern an instantaneous error $e_i(n)$ is defined by

$$e_j(n) = d_j(n) - y_j(n) \quad (4.1)$$

Using the theory of gradient descent learning, each weight in the network can be modified by correcting the present value of the weight with a term that is proportional to the present input and error at the weight, i.e.

$$w_{ij}(n+1) = w_{ij}(n) + \eta \delta_i(n) x_j(n) \quad (4.2)$$

The local error $\delta_i(n)$ can be directly computed from $e_i(n)$ at the output PE or can be computed as a weighted sum of errors at the internal PEs. The constant η is called the learning rate. Lower the value of η more accurately the system is trained. This procedure is called the back propagation algorithm. Back propagation computes the sensitivity of a cost functional with respect to each weight in the network, and updates each weight according to the sensitivity. The

beauty of the network structure is that it can be implemented with local information and requires just a few multiplications per weight, which is very efficient [7]. As this is a gradient descent procedure, it only uses the local information so that it can be caught local minima easily. Moreover, the procedure is inherently noisy since we are using a poor estimate of the gradient, causing slow convergence. Momentum learning is an improvement to the straight gradient descent in the sense that a memory term (the past increment to the weight) is used to speed up and stabilize convergence. The momentum factor (α) normally lies between 0.1 and 0.9.

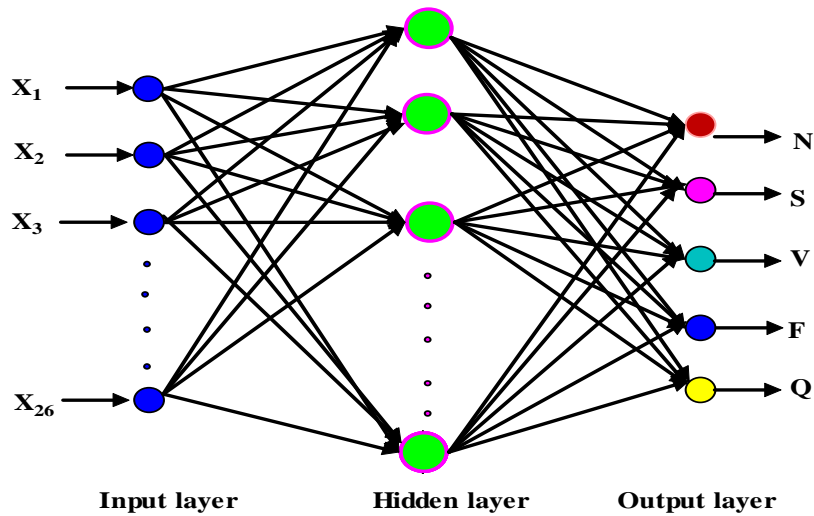


Fig. 4.1 General Structure of multilayer neural network.

4.3 Radial basis function neural network (RBFNN)

Radial basis function neural network (RBFNN) is a widely used pattern recognition tasks due to its fast learning algorithms. RBFNNs are nonlinear hybrid network which is a three layer structure. Generally the RBF network contains one hidden layer only. Fig. 2 shows the general structure of the RBFNN. The input layer provides the information from the input vector to each of the nodes in the hidden layer. Each node in the hidden layer then find out the radial distance from center to each point on the associated radial basis function. Finally, each node in the output layer computes a linear combination of the activations of the hidden nodes [23]. The general mathematical form of the output nodes in an RBFNN is as follows:

$$c_j(x) = \sum_{i=1}^k w_{ji} \exp\left(-\frac{\|x - \mu_i\|^2}{\sigma_i^2}\right) \quad (4.3)$$

where $c_j(x)$ is the function corresponding to the j^{th} output unit (class- j) and is a linear combination of k radial basis functions $\phi(\cdot)$ with center μ_i and bandwidth σ_i . Also, w_j is the weight vector of class- j and w_{ji} is the weight corresponding to the j^{th} class and i^{th} center.

In pattern recognition problems usually a Gaussian function is used as the basis function of the RBFNN [23]. So, the Eq. (4.3) becomes:

$$c_j(x) = \sum_{i=1}^k w_{ji} \exp\left(-\frac{\|x - \mu_i\|^2}{2\sigma_i^2}\right) \quad (4.4)$$

From the Eq. (4.4) it can be clearly seen that the output of the RBFNN is dependent to the total number of neurons k , the weights between the output and the hidden layer of the network w_{ji} , centers of the each neuron μ_i and finally bandwidth of the each neuron σ_i . So the classification performance of the RBFNN lies in determining the correct parameters for the network that means (center and spread).

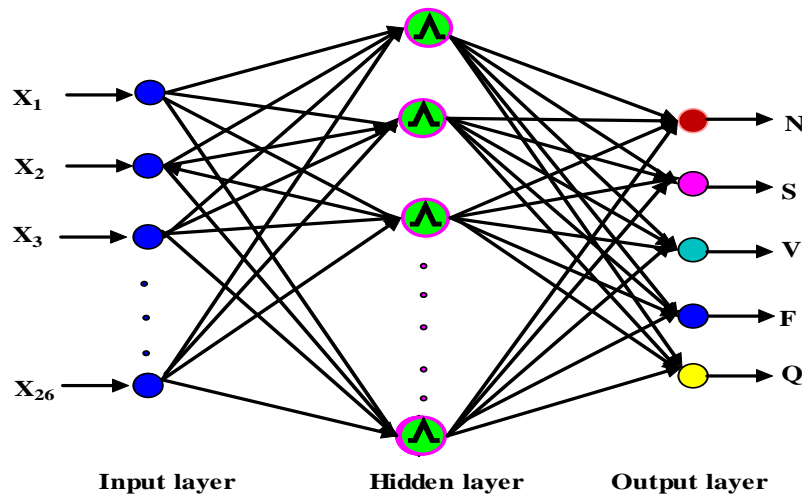


Fig. 4.2 General structure of the radial basis function neural network.

The centers and widths of the RBFNN are the two parameters which can affect the classification performance. Several methods have been proposed to find the centers of the RBFNN. These are usually clustering based methods that find center locations between the input feature vector locations or some of the input feature vectors directly can be used as the centers of the neurons. Hence it has been confirmed that the best center locations may not be necessarily

located inside the input feature vectors. The most common algorithm to determine the neuron centers of the RBFNN are the K-Means algorithm.

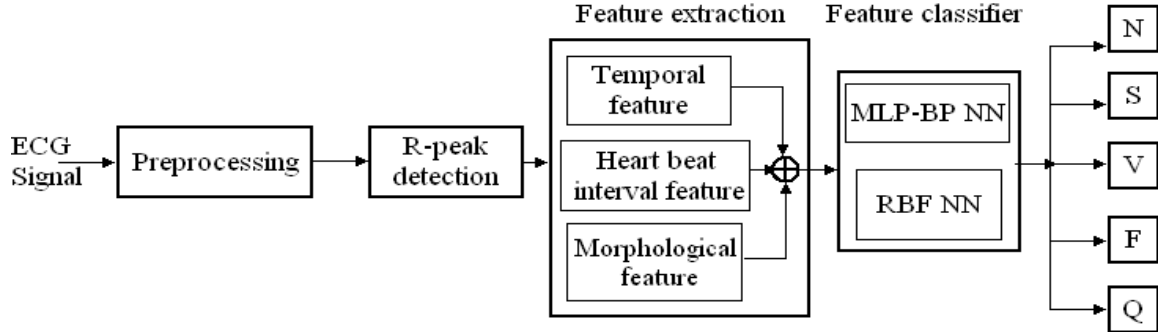


Fig. 4.3 Block diagram representation of ECG beat classifier.

4.4 Performance matrix

The performance of the classifier is estimated four statistical indices [22]: classification accuracy (Acc), sensitivity (Se), specificity (Sp), and positive predictivity (Pp), which are defined in the following Eqs. (4.5) – (4.8), respectively.

1. Classification Accuracy (Acc)

Classification accuracy measures the overall system performance over all classes of beats. It is the ratio of correctly classified patterns to the total number of pattern classified.

$$Acc(\%) = \frac{TP + TN}{TP + TN + FP + FN} \times 100 \quad (4.5)$$

2. Sensitivity (Se)

It is the ratio of correctly classified event among all events.

$$Se(\%) = \frac{TP}{TP + FN} \times 100 \quad (4.6)$$

3. Specificity (Spe)

The specificity is the ratio of the number of correctly rejected nonevents, TN (true negatives), to the total number of nonevents and is given by

$$Spe(\%) = \frac{TN}{TN + FP} \times 100 \quad (4.7)$$

4. Positive predictivity (Ppr)

Positive predictivity is the ratio of the number of correctly detected events, TP, to the total number of events detected by the analyzer and is given by

$$Ppr(\%) = \frac{TP}{TP + FP} \times 100 \quad (4.8)$$

Where, TP = Number of true positive beat detected

FP = Number of false positive beat

FN = Number of false negative beat

TN = Number of true negative beat

4.5 Classification Performance

The classification performance are analyzed on 24 records of the MIT/BIH arrhythmia database, which includes a total of 49473 beats to be classified into five heartbeat types following the AAMI convention. The 24 records are taken from the #tape numbered in the range of 200–234 which contain complex ventricular, junctional, and supraventricular arrhythmias. For the classification experiments, the common part of the training dataset contains a total of 244 representative beats, including 75 from each type-N, -S, and -V beats, and all (13) type-F and (6) type-Q beats, randomly sampled from each class from the first 20 records (picked from the range 100–124) of the MIT/BIH database. The patient-specific training data include the beats from the first 5 min of the corresponding patient’s ECG record. Hence Patient specific feed forward MLP networks and radial basis function neural networks are trained with a total of 244 common training beats and along with first 5 min of the corresponding patient’s ECG record. The remaining beats (25 min) of 24 records, which contains pathological cases are completely new to the classifier, and are used as test patterns for performance evaluation. The neural network target output is set according to table 4.1.

Table 4.1 ECG classes and representation of desired neural network output

Classes	ECG beat description	Neural network output				
1	Normal beat (N)	0	0	0	0	1
2	Supraventricular ectopic beat (S)	0	0	0	1	0
3	ventricular ectopic beat (V)	0	0	1	0	0
4	Fusion beat (F)	0	1	0	0	0
5	Unknown beat (Q)	1	0	0	0	0

Table 4.2 Comprehensive results for testing files of 24 records in MIT/BIH arrhythmia database

MIT-BIH record	No. of beats used in testing					Supraventricular ectopic beat (S)				ventricular ectopic beat (V)				Supraventricular ectopic beat (S)				ventricular ectopic beat (V)				
	N	S	V	F	Q	TP	FP	FN	TN	TP	FP	FN	TN	Acc (%)	Se (%)	Spe (%)	Ppr (%)	Acc (%)	Se (%)	Spe (%)	Ppr (%)	
200*	1431	26	693	1	0	18	21	8	2075	655	11	38	1146	98.6	69.2	99.0	46.2	97.4	94.5	99.0	98.3	
201	1193	108	198	2	0	6	71	102	1323	106	119	92	1186	88.5	5.6	94.9	7.8	86.0	53.5	90.9	47.1	
202*	1800	47	10	1	0	8	136	39	1675	5	51	5	1802	90.6	17.0	92.5	5.6	97.0	50.0	97.2	8.9	
203	2092	2	401	1	1	0	18	2	2477	257	14	144	2083	99.2	0.0	99.3	0.0	93.7	64.1	99.3	94.8	
205	2070	2	64	10	0	2	6	0	2138	55	4	9	2078	99.7	100.0	99.7	25.0	99.4	85.9	99.8	93.2	
207	1375	107	109	0	0	58	11	49	1473	8	27	101	1455	96.2	54.2	99.3	84.1	92.0	7.3	98.2	22.9	
208	1310	2	804	297	2	1	25	1	2388	784	23	20	1590	98.9	50.0	99.0	3.8	98.2	97.5	98.6	97.1	
209	2148	374	1	0	0	216	13	158	2151	0	8	1	2522	93.3	57.8	99.4	94.3	99.6	0.0	99.7	0.0	
210*	1966	15	122	6	0	4	11	11	2086	90	10	32	1978	99.0	26.7	99.5	26.7	98.0	73.8	99.5	90.0	
212*	2567	0	0	0	0	0	0	0	0	0	0	0	0	NaN	NaN	NaN	NaN	NaN	NaN	NaN	NaN	
213*	2211	27	69	258	0	7	15	20	2523	26	31	43	2465	98.6	25.9	99.4	31.8	97.1	37.7	98.8	45.6	
214*	1667	0	207	1	1	0	0	0	0	189	7	18	1661	NaN	NaN	NaN	NaN	98.7	91.3	99.6	96.4	
215	2666	2	119	0	0	2	5	0	2780	110	6	9	2662	99.8	100.0	99.8	28.6	99.5	92.4	99.8	94.8	
219*	1714	7	51	0	0	0	0	7	1765	45	7	6	1714	99.6	0.0	100.0	NaN	99.3	88.2	99.6	86.5	
220	1600	93	0	0	0	66	7	27	1593	0	0	0	0	98.0	71.0	99.6	90.4	NaN	NaN	NaN	NaN	
221*	1701	0	304	0	0	0	0	0	0	291	4	13	1697	NaN	NaN	NaN	NaN	99.2	95.7	99.8	98.6	
222*	1900	207	0	0	0	145	312	62	1582	0	0	0	0	82.2	70.0	83.5	31.7	NaN	NaN	NaN	NaN	
223	1659	61	386	8	0	52	90	9	1963	234	102	152	1728	95.3	85.2	95.6	36.6	88.5	60.6	94.4	69.6	
228*	1395	3	352	0	0	1	8	2	1739	330	5	22	1393	99.4	33.3	99.5	11.1	98.5	93.8	99.6	98.5	
230	1858	0	1	0	0	0	0	0	0	0	1	1	1857	NaN	NaN	NaN	NaN	99.9	0.0	99.9	0.0	
231*	1277	1	2	0	0	0	0	1	1279	2	0	0	1278	99.9	0.0	100.0	NaN	100.0	100.0	100.0	100.0	
232*	319	1165	0	0	0	1157	8	8	311	0	0	0	0	98.9	99.3	97.5	99.3	NaN	NaN	NaN	NaN	
233*	1853	4	673	6	0	4	8	0	2524	655	13	18	1850	99.7	100.0	99.7	33.3	98.8	97.3	99.3	98.1	
234*	2237	50	0	0	0	11	0	39	2237	0	0	0	0	98.3	22.0	100.0	100.0	NaN	NaN	NaN	NaN	
Total	42009	2303	4566	591	4									Average	96.7	49.4	97.9	42.0	96.9	67.6	98.6	70.6

Table 4.3 Summary table of beat-by-beat classification of 24 records in MIT/BIH arrhythmia database

		ALGOTITHM				
		n	s	v	f	q
TRUTH	N	40613	596	357	421	22
	S	373	1758	155	11	6
	V	448	162	3842	109	5
	F	94	9	38	450	0
	Q	1	1	1	1	0

Table 4.4 Classification performance of 24 records in MIT/BIH arrhythmia database

TP	FP	FN	TN	Acc (%)	Se (%)	Spe (%)	Ppr (%)
40613	916	1759	6549	94.6	95.8	87.7	97.8
1758	768	545	46402	97.3	76.3	98.4	69.6
3842	551	724	44356	97.4	84.1	98.8	87.5
450	542	141	48340	98.6	76.1	98.9	45.4
0	33	4	49436	99.9	0.0	99.9	0.0
Average				97.6	66.5	96.7	60.0

Table4.5 SVEB result for testing files of 14 records in MIT/BIH arrhythmia database using MLP

MIT-BIH record	No. of beats used in testing					Supraventricular ectopic beat (S)				Supraventricular ectopic beat (S)			
	N	S	V	F	Q	TP	FP	FN	TN	Acc (%)	Se (%)	Spe (%)	Ppr (%)
200*	1431	26	693	1	0	18	21	8	2075	98.6	69.2	99.0	46.2
202*	1800	47	10	1	0	8	136	39	1675	90.6	17.0	92.5	5.6
210*	1966	15	122	6	0	4	11	11	2086	99.0	26.7	99.5	26.7
213*	2211	27	69	258	0	7	15	20	2523	98.6	25.9	99.4	31.8
214*	1667	0	207	1	1	0	0	0	0	NaN	NaN	NaN	NaN
219*	1714	7	51	0	0	0	0	7	1765	99.6	0.0	100.0	NaN
221*	1701	0	304	0	0	0	0	0	0	NaN	NaN	NaN	NaN
228*	1395	3	352	0	0	1	8	2	1739	99.4	33.3	99.5	11.1
231*	1277	1	2	0	0	0	0	1	1279	99.9	0.0	100.0	NaN
233*	1853	4	673	6	0	4	8	0	2524	99.7	100.0	99.7	33.3
234*	2237	50	0	0	0	11	0	39	2237	98.3	22.0	100.0	100.0
212*	2567	0	0	0	0	0	0	0	0	NaN	NaN	NaN	NaN
222*	1900	207	0	0	0	145	312	62	1582	82.2	70	83.5	31.7
232*	319	1165	0	0	0	1157	8	8	311	98.9	99.3	97.5	99.3
Average										96.8	42.1	97.3	42.8

NaN: Not a Number

Table 4.6 VEB result for testing files of 11 records in MIT/BIH arrhythmia database using MLP

MIT-BIH record	No. of beats used in testing					Ventricular ectopic beat (V)				Ventricular ectopic beat (V)			
	N	S	V	F	Q	TP	FP	FN	TN	Acc (%)	Se (%)	Spe (%)	Ppr (%)
200*	1431	26	693	1	0	655	11	38	1146	97.4	94.5	99.0	98.3
202*	1800	47	10	1	0	5	51	5	1802	97.0	50.0	97.2	8.9
210*	1966	15	122	6	0	90	10	32	1978	98.0	73.8	99.5	90.0
213*	2211	27	69	258	0	26	31	43	2465	97.1	37.7	98.8	45.6
214*	1667	0	207	1	1	189	7	18	1661	98.7	91.3	99.6	96.4
219*	1714	7	51	0	0	45	7	6	1714	99.3	88.2	99.6	86.5
221*	1701	0	304	0	0	291	4	13	1697	99.2	95.7	99.8	98.6
228*	1395	3	352	0	0	330	5	22	1393	98.5	93.8	99.6	98.5
231*	1277	1	2	0	0	2	0	0	1278	100.0	100.0	100.0	100.0
233*	1853	4	673	6	0	655	13	18	1850	98.8	97.3	99.3	98.1
234*	2237	50	0	0	0	0	0	0	0	NaN	NaN	NaN	NaN
									Average	98.4	82.2	99.2	82.1

Table 4.7 SVEB result for testing files of 14 records in MIT/BIH arrhythmia database using RBF

MIT-BIH record	No. of beats used in testing					Supraventricular ectopic beat (S)				Supraventricular ectopic beat (S)			
	N	S	V	F	Q	TP	FP	FN	TN	Acc (%)	Se(%)	Spe(%)	Ppr(%)
200*	1431	26	693	1	0	14	71	12	2054	96.14	53.85	0.66	16.47
202*	1800	47	10	1	0	37	540	10	1271	70.40	78.72	2.04	6.41
210*	1966	15	122	6	0	6	76	9	2018	95.97	40.00	0.29	7.32
212*	2567	0	0	0	0	0	233	0	2334	90.92	NaN	0.00	0.00
213*	2211	27	69	258	0	16	142	11	2396	59.26	59.26	0.63	10.13
214*	1667	0	207	1	1	0	86	0	1790	NaN	NaN	0.00	0.00
219*	1714	7	51	0	0	3	96	4	1669	42.86	42.86	0.17	3.03
221*	1701	0	304	0	0	0	96	0	1909	NaN	NaN	0.00	0.00
222*	1900	207	0	0	0	195	83	12	1817	94.20	94.20	10.26	70.14
228*	1395	3	352	0	0	3	10	0	1737	100.00	100.00	0.17	23.08
231*	1277	1	2	0	0	1	17	0	1262	100.00	100.00	0.08	5.56
232*	319	1165	0	0	0	1026	20	139	299	88.07	88.07	321.63	98.09
233*	1853	4	673	6	0	4	157	0	2375	100.00	100.00	0.16	2.48
234*	2237	50	0	0	0	26	81	24	2156	52.00	52.00	1.16	24.30
									Average	82.49	73.54	30.66	24.27

Table 4.8 VEB result for testing files of 11 records in MIT/BIH arrhythmia database using RBF

MIT-BIH record	No. of beats used in testing					Ventricular ectopic beat (V)				Ventricular ectopic beat (V)			
	N	S	V	F	Q	TP	FP	FN	TN	Acc (%)	Se (%)	Spe (%)	Ppr (%)
200*	1431	26	693	1	0	606	6	87	1452	95.68	87.45	41.56	99.0
202*	1800	47	10	1	0	8	44	2	1804	97.52	80.00	0.43	15.4
210*	1966	15	122	6	0	94	110	8	1897	94.40	92.16	4.68	46.1
213*	2211	27	69	258	0	34	131	35	2365	93.53	49.28	1.36	20.6
214*	1667	0	207	1	1	119	3	88	1666	95.15	57.49	7.13	97.5
219*	1714	7	51	0	0	49	27	2	1694	98.36	96.08	2.85	64.5
221*	1701	0	304	0	0	252	2	52	1699	97.31	82.89	14.81	99.2
228*	1395	3	352	0	0	339	3	13	1395	99.09	96.31	24.25	99.1
231*	1277	1	2	0	0	0	1	2	1277	99.77	0.00	0.00	0.0
233*	1853	4	673	6	0	516	7	157	1856	93.53	76.67	27.70	98.7
234*	2237	50	0	0	0	0	13	0	2274	99.43	NaN	NaN	NaN
Average										96.7	71.8	12.5	64.0

Table 4.9 SVEB and VEB comparison result are based on 14 and 11 common testing records respectively

Methods	Supraventricular ectopic beat (S)				ventricular ectopic beat (V)			
	Acc (%)	Se (%)	Spe (%)	Ppr (%)	Acc (%)	Se (%)	Spe (%)	Ppr (%)
Hu et al.[5]	N/A	N/A	N/A	N/A	94.8	78.9	96.8	75.8
Chazal et al. [4]	92.4	76.4	93.2	38.7	96.4	77.5	98.9	90.6
Jiang and Kong [2]	97.5	74.9	98.8	78.8	98.8	94.3	99.4	95.8
Ince et al. [1]	96.1	81.8	98.5	63.4	97.9	90.3	98.8	92.2
MLP BP NN method	98.2	32.7	98.8	36.4	98.4	82.2	99.2	82.1
RBF detected method	82.5	73.5	30.7	24.3	96.7	71.8	12.5	64.0

N/A: Not Analyzed

Table 4.10 VEB and SVEB comparison result are based on 24 common testing records

Methods	Supraventricular ectopic beat (S)				ventricular ectopic beat (V)			
	Acc (%)	Se(%)	Spe(%)	Ppr(%)	Acc (%)	Se(%)	Spe(%)	Ppr(%)
Jiang and Kong [2]	96.6	50.6	98.8	67.9	98.1	86.6	99.3	93.3
Ince et al. [1]	96.1	62.2	98.5	56.7	97.6	83.4	98.1	87.4
ANN detected method	96.7	49.4	97.9	42	96.9	67.6	98.6	70.6

Table 4.2 summarizes beat-by-beat classification results of ECG heartbeat patterns for 24 test records. Classification performance is measured using the four standard metrics: classification accuracy (*Acc*), sensitivity (*Sen*), specificity (*Spe*), and positive predictivity (*Ppr*). The MLP neural network and RBF neural network are compared with three existing algorithms, [1], [2], [3] and [5], which comply with the AAMI standards and use all records from the MIT/BIH arrhythmia database. For comparing the performance results, the problem of VEB and SVEB detection is considered individually. The performance results for VEB detection in the first four rows of Table 4.9 are based on 11 test recordings (200, 202, 210, 213, 214, 219, 221, 228, 231, 233, and 234) that are common to all four methods. For SVEB detection, comparison results are based on 14 common recordings (with the addition of records 212, 222, and 232). It is observed that the MLP neural network classifier achieves comparable performance over the training and testing set of patient records as compared to existing method [1] and [2]. It is worth noting that the number of training beats used for each patient’s classifier was less than 2% of all beats in the training dataset. Experimental result shows that the MLP –BP neural network achieves better result as compared to RBF network.

4.6 Conclusion

The ECG signal can be used as a reliable indicator of heart diseases. The MLP neural network and RBF neural network classifiers are presented as the diagnostic tool to aid the

physician in the analysis of cardiac abnormalities. The most important factor in determining whether an automatic ECG diagnosis system is successful or not is the accuracy of event detection. The accuracy of the tools depends on several factors, such as the size and quality of the training set, the efficient extracted feature set and also the parameters chosen to represent the input. The experimental result shows that the MLP BP NN achieves sensitivity of 98.2% and 98.4% for SVEBs and VEBs respectively. For the same number of test set the RBF NN shows sensitivity 82.5% and 96.7% for SVEBs and VEBs respectively. Hence the MLP neural network shows better result as compared to RBF neural network.

References

- [1] T.Ince, S. Kiranyaz, and M. Gabbouj, "A generic and robust system for automated patient-specific classification of ECG signals," *IEEE Trans. Biomed. Eng.* vol. 56, pp. 1415-1426, 2009.
- [2] W. Jiang and S. G. Kong, "Block-based neural networks for personalized ECG signal classification," *IEEE Trans. Neural Netw.*, vol. 18, no. 6, pp. 1750–1761, Nov. 2007.
- [3] S. Osowski, T. H. Linh, and T. Markiewicz, "Support vector machinebased expert system for reliable heart beat recognition," *IEEE Trans. Biomed. Eng.*, vol. 51, no. 4, pp. 582–589, Apr. 2004.
- [4] P.de Chazal, M.O. Duyer, and R.B. Reilly, "Automatic classification of heartbeat using ECG morphology and heart beat interval features," *IEEE Trans. Biomed. Eng.* vol. 51, pp. 1196-1206, 2004.
- [5] Y. Hu, S. Palreddy, and W. J. Tompkins, "A patient-adaptable ECG beat classifier using a mixture of experts approach," *IEEE Trans. Biomed. Eng.*, vol. 44, no. 9, pp. 891–900, Sep. 1997.
- [6] P. de Chazal, R.B. Reilly, "A patient-adapting heartbeat classifier using ECG morphology and heartbeat interval feature," *IEEE Trans. Biomed. Eng.* vol. 53, pp. 2535-2543, 2006.
- [7] Simon Haykin, *Neural networks a comprehensive foundation*, Pearson Prentice Hall, pp.178-330.
- [8] MIT-BIH Database distribution, Massachusetts Institute of Technology, 77 Massachusetts Avenue, Cambridge, MA 02139,1998.<http://www.physionet.org/physiobank/database/mitdb/>
- [9] American National Standard for Ambulatory Electrocardiographs, publication ANSI/AAMI EC38-1994, Association for the Advancement of Medical Instrumentation, 1994.
- [10]D. A. Coast, R. M. Stern, G. G. Vano and S. A. Biller, "An approach to cardiac arrhythmia analysis using Hidden Markov Model, " *IEEE Trans. Biomed. Eng.* ,vol. 37, no. 9,Sep. 1990.

- [11] R. J. Schalkoff, "Pattern Recognition: Statistical, Structural, and Neural Approaches", JOHN WILEY & SONS, INC., 1992.
- [12] T. H. Yeap, F. Johnson, and M. Rachniowski, "ECG beat classification by a neural network," in *Proc. Annu. Int. Conf. IEEE Engineering Medicine and Biology Society*, 1990, pp. 1457–1458.
- [13] Y. H. Hu, W. J. Tompkins, J. L. Urrusti, and V. X. Afonso, "Applications of artificial neural networks for ECG signal detection and classification," *J. Electrocardiol.*, vol. 26, pp. 66–73, 1993.
- [14] S. Osowski and T. L. Linh, "ECG beat recognition using fuzzy hybrid neural network," *IEEE Trans. Biomed. Eng.*, vol. 48, no. 11, pp. 1265–1271, Nov. 2001.
- [15] I. Christov, I. Jekova, and G. Bortolan, "Premature ventricular contraction classification by the kth nearest-neighbours rule," *Physiol. Meas.*, vol. 26, pp. 123–130, 2005.
- [16] S. Evans, H. Hastings, and M. Bodenheimer, "Differentiation of beats of ventricular and sinus origin using a self-training neural network," *PACE*, vol. 17, pp. 611–626, 1994.
- [17] Recommended Practice for Testing and Reporting Performance Results of Ventricular Arrhythmia Detection Algorithms, 1987. Association for the Advancement of Medical Instrumentation.
- [18] B. D. Ripley, *Pattern Recognition and Neural Networks*, Cambridge, U.K.: Cambridge Univ. Press, 1996.
- [19] P. de Chazal and R. B. Reilly, "A comparison of the ECG classification performance of different feature sets," *Proc. Comput. Cardiology*, vol. 27, pp. 327–330, 2000.
- [20] T. H. Linh, S. Osowski, and M. Stodolski, "On-line heart beat recognition using Hermite polynomials and neuro-fuzzy network," *IEEE Trans. Instrum. Meas.*, vol. 52, no. 4, pp. 1224–1231, Aug. 2003.
- [21] X. Yao, "Evolving artificial neural networks," *Proc. IEEE*, vol. 87, no. 9, pp. 1423–1447, Sep. 1999.
- [22] A. E. Zadeh, A. Khazaei, and V. Ranaei, "classification of electrocardiogram signal using supervised classifier and efficient features," *Computer methods and Programs in Biomedicine*, vol. 99, pp. 179-194, 2010.
- [23] M. Korurek and B. Dogan. "ECG beat classification using particle swarm optimization and radial basis function neural network," *Expert System with Application*, vol. 33, pp. 7563-7569, 2010.
- [24] R. O. Duda, P. E. Hart, and D. G. Stork, *Pattern Recognition*, 2nd ed. New York: Wiley, 2000.

CHAPTER 5

Conclusion and Future work

5.1 Conclusion

This thesis provides an algorithm for accurate detection of QRS complex and automatic classification of cardiac arrhythmias recommended by Association for the Advancement of Medical Instrumentation (AAMI). Feature extraction methodology proves an essential process for reducing the inputs to the classifier drastically. The automatic classification of arrhythmias helps in recognizing the diseases more accurately with less time.

- Chapter 2 of this thesis represents a novel algorithm for detection of QRS complex in ECG signal. Accurate detection of QRS complex is the first and most important part of ECG signal analysis. A novel approach using the properties of Hilbert transform and autocorrelation function is developed. The autocorrelation based method is used to find out the period of one cardiac cycle. The high slope point that means R-peak in ECG signal is identified from the envelope of Hilbert transform output. The adaptive threshold technique is used which helps in distinguish the R-peaks from P-wave and T-wave. The beat detection algorithm is compared with the two existing techniques like Pan-Tompkins [1], difference operation method (DOM) [2]. The experimental result shows that the proposed method performs better result as compared to PT- method and DOM- method.
- Chapter 3 of this thesis represents the feature extraction methodology for each heartbeat of one cardiac cycle. The morphological features combined with temporal features of each heartbeat are extracted to provide better classification accuracy. The feature extraction methodology extracts the features of each heartbeat after automatic detection of R-peak. This method does not follow the beat annotation file provided by the exports as references of finding R-peaks. Hence it can also be applicable in real time application. Thus the feature extraction techniques play a vital role in the performance of classifying beta arrhythmias using the classifiers.
- Chapter 4 of this thesis represents the automatic classification of cardiac arrhythmias heartbeats into five classes: normal beats, VEBs, SVEBs, fusion beats and unclassified beats. The combination of local classifier of each patient with the

global classifier performs better classification result than individual. The classification performance of 11 #tapes contain VEBs and 14 #tapes hold SVEBs are compared with the earlier existing methods [3]-[6]. The performance also analyzed using 24 #tapes of MIT-BIH arrhythmias database and compared with methods [4], [5]. The comparative study of ECG beat classifier using multilayer perceptron neural network and radial basis function neural network has done and the result shows MLP neural network achieve higher classification accuracy than RBF neural network.

5.2 Future scope

Automatic cardiac abnormality classification is necessary for real time application. The classification accuracy can improve by extracting the better features of ECG signal. Future developments can be made as follows

- To design better feature extraction methodology which can improve the classification result of cardiac arrhythmias in ECG signal.
- To analyze the classification accuracy using different classifier such that it can classify the beat arrhythmias in the approved manner.
- To modify the network structure according to cost function of multilayer neural network so that it can achieve better classification accuracy as compared to existing ECG beat classifier.
- Real time operation for recognizing the cardiac arrhythmias can also be done since the methodology uses the automatic detection of R-peaks and feature extraction techniques.

5.3 References

- [1] J. Pan, W. J. Tompkins, "A real time QRS detection algorithm," *IEEE Trans. Biomed. Eng.*, vol. 32, pp. 230–236, 1985.
- [2] Y.C. Yeha, and W. J. Wang, "QRS complexes detection for ECG signal The Difference Operation Method (DOM)," *Computer methods and programs in biomedicine*, vol. 9, pp. 245–254, 2008.
- [3] P.de Chazal, M.O. Duyer, and R.B. Reilly, "Automatic classification of heartbeat using ECG morphology and heart beat interval features," *IEEE Trans. Biomed. Eng.* vol. 51, pp. 1196-1206, 2004.

- [4] T. Ince, S. Kiranyaz, and M. Gabbouj, "A generic and robust system for automated patient-specific classification of ECG signals," *IEEE Trans. Biomed. Eng.* vol. 56, pp. 1415-1426, 2009.
- [5] W. Jiang and S. G. Kong, "Block-based neural networks for personalized ECG signal classification," *IEEE Trans. Neural Netw.*, vol. 18, no. 6, pp. 1750–1761, Nov. 2007.
- [6] Y. Hu, S. Palreddy, and W. J. Tompkins, "A patient-adaptable ECG beat classifier using a mixture of experts approach," *IEEE Trans. Biomed. Eng.*, vol. 44, no. 9, pp. 891–900, Sep. 1997.

List of Publications

1. **J.P. Sahoo**, M.K. Das, S. Ari and S. Behera, “Autocorrelation and Hilbert transform based QRS Complex detection in ECG Signal,” *International Journal of Signal and Imaging Systems Engineering*, (In Press).
2. **J.P. Sahoo**, S. Behera, and S. Ari, “A novel technique for QRS complex detection in ECG signal based on Hilbert transform and autocorrelation,” *International Conference on Electronic Systems*, NIT, Rourkela, Jan 7-9, 2011.
3. M.K. Das, S. Ari and **J.P. Sahoo**, “Enhancement of Electrocardiogram Signal using S-Transform,” *IEEE TENCON*, Bali, Indonesia, November 21-24, 2011(Communicated).